NAVAL
POSTGRADUATE
SCHOOL

MONTEREY, CALIFORNIA

THESIS

EXPERIMENTAL VERIFICATION OF THE FLOW AROUND COMPRESSOR BLADES IN CASCADE AT STALL WITH INITIAL NUMERICAL SIMULATIONS

by

Michael A. Glova

March, 2006

Thesis Advisor:	Garth V. Hobson
Second Reader:	Knox T. Millsaps

Approved for public release; distribution is unlimited

REPORT DOCUMENTATION PAGE			*Form Approved OMB No. 0704-0188*
Public reporting burden for this collection of information is estimated to average 1 hour per response, including the time for reviewing instruction, searching existing data sources, gathering and maintaining the data needed, and completing and reviewing the collection of information. Send comments regarding this burden estimate or any other aspect of this collection of information, including suggestions for reducing this burden, to Washington headquarters Services, Directorate for Information Operations and Reports, 1215 Jefferson Davis Highway, Suite 1204, Arlington, VA 22202-4302, and to the Office of Management and Budget, Paperwork Reduction Project (0704-0188) Washington DC 20503.			
1. AGENCY USE ONLY *(Leave blank)*	**2. REPORT DATE** March 2006	**3. REPORT TYPE AND DATES COVERED** Master's Thesis	
4. TITLE AND SUBTITLE: Experimental Verification of the Flow Around Compressor Blades in Cascade at Stall with Initial Numerical Simulations			**5. FUNDING NUMBERS**
6. AUTHOR(S) Glova, Michael A			
7. PERFORMING ORGANIZATION NAME(S) AND ADDRESS(ES) Naval Postgraduate School Monterey, CA 93943-5000			**8. PERFORMING ORGANIZATION REPORT NUMBER**
9. SPONSORING /MONITORING AGENCY NAME(S) AND ADDRESS(ES) N/A			**10. SPONSORING/MONITORING AGENCY REPORT NUMBER**
11. SUPPLEMENTARY NOTES The views expressed in this thesis are those of the author and do not reflect the official policy or position of the Department of Defense or the U.S. Government.			
12a. DISTRIBUTION / AVAILABILITY STATEMENT Approved for public release; distribution is unlimited			**12b. DISTRIBUTION CODE**

13. ABSTRACT (maximum 200 words)

The flow around second-generation controlled diffusion blades in cascade at stall was examined experimentally through the use of a two-component laser-Doppler velocimeter (LDV). The experimental results were compared with computational fluid dynamics predictions in order to provide information that will allow for more exact design of advanced blades. Midspan blade surface pressure data were also collected over a range of Reynolds numbers based on chord of 270,000 to 720,000. Pressure distribution plots verified that the blades were in the stalled condition. The LDV measurement surveys were taken at one inlet station, at three stations on the suction side of the blade, and at three stations in the wake.

14. SUBJECT TERMS Controlled-Diffusion, Compressor, Stator, Cascade, Laser Doppler Velocimetry, Computational Fluid Dynamics			**15. NUMBER OF PAGES** 86
			16. PRICE CODE
17. SECURITY CLASSIFICATION OF REPORT Unclassified	**18. SECURITY CLASSIFICATION OF THIS PAGE** Unclassified	**19. SECURITY CLASSIFICATION OF ABSTRACT** Unclassified	**20. LIMITATION OF ABSTRACT** UL

THIS PAGE INTENTIONALLY LEFT BLANK

EXPERIMENTAL VERIFICATION OF THE FLOW AROUND COMPRESSOR BLADES IN CASCADE AT STALL WITH INITIAL NUMERICAL SIMULATIONS

Michael A. Glova
Lieutenant Commander, United States Navy
B.S. History, United States Naval Academy, 1996

Submitted in partial fulfillment of the
requirements for the degree of

MASTER OF SCIENCE IN MECHANICAL ENGINEERING

from the

**NAVAL POSTGRADUATE SCHOOL
March 2006**

Author: Michael A. Glova

Approved by: Garth V. Hobson
              Thesis Advisor

              Knox T. Millsaps
              Second Reader

              Anthony J. Healy
              Chairman, Department of Mechanical and
              Astronautical Engineering

THIS PAGE INTENTIONALLY LEFT BLANK

ABSTRACT

The flow around second-generation controlled diffusion blades in cascade at stall was examined experimentally through the use of a two-component laser-Doppler velocimeter (LDV). The experimental results were compared with computational fluid dynamics predictions in order to provide information that will allow for more exact design of advanced blades. Midspan blade surface pressure data were also collected over a range of Reynolds numbers based on chord of 270,000 to 720,000. Pressure distribution plots verified that the blades were in the stalled condition. The LDV measurement surveys were taken at one inlet station, at three stations on the suction side of the blade, and at three stations in the wake.

THIS PAGE INTENTIONALLY LEFT BLANK

TABLE OF CONTENTS

LIST OF FIGURES

THIS PAGE INTENTIONALLY LEFT BLANK

LIST OF SYMBOLS

c	blade chord (m)
C_{ac}	fraction of axial chord
h	blade span (m)
Re	Reynolds number
Re_c	Reynolds number based on blade chord
S	blade spacing (m)
U	axial velocity component (m/s)
V	tangential velocity component (m/s)
V_{ref}	reference velocity (test section inlet velocity) (m/s)
X	dimensionless velocity
X'	traverse coordinate position (m)
Y'	traverse coordinate location (m)
Z'	traverse coordinate station (m)
y/S	non-dimensionalized pitchwise direction
$k/(V_{ref}^2)$	non-dimensionalized total turbulence kinetic energy
U_{tot}	total velocity (with components U,V,W)
β_1	tunnel inlet flow angle
δ	boundary layer thickness

THIS PAGE INTENTIONALLY LEFT BLANK

ACKNOWLEDGMENTS

Many people deserve special mention for their invaluable support to me during this project. First of all I thank Professor Garth V. Hobson for his guidance and patience; but most of all for knowledge that he most willingly passed along to me.

I also thank my parents for raising me to work hard, play fairly, and to always put other peoples' needs before my own.

Next I thank my wife Janelle, daughter Analia, and son Michael. You all have been most supportive of my education and very understanding while I have needed to be away conducting my research.

Finally, I wish to send a message to my late father…"It looks like we were both right."

THIS PAGE INTENTIONALLY LEFT BLANK

I. INTRODUCTION

A. BACKGROUND

Advances in engine technology made engine designs more efficient and cost effective to both manufacture and operate. One of the most significant improvements to compressor design was the advent of controlled-diffusion (CD) compressor blading. Numerical fluid flow prediction techniques, specifically Computational Fluid Dynamics (CFD) codes, greatly enhanced compressor blade design technology. The main advantage of CD blades over earlier pedigree blade designs was that their unique geometry of the suction side of the blades allowed for greater turning and delayed onset of stall. As a result of the high turning angles, CD blades provided more lift than conventional blading. Thus, engines with fewer blades, and thus lower production costs, produced the same thrust as legacy engine types.

The CD blades investigated in this study were a second generation 67B series blades designed at what is today NASA Glenn Research Facility. They were the first improvement over 67A compressor blades, also NASA designed. The Turbopropulsion Laboratory (TPL) at the Naval Postgraduate School (NPS) conducted research on 67B blades in linear cascade for the past 11 years, starting with Hansen [Ref 1]. Hansen experimentally and computationally studied flow at the design inlet flow angle (β_1) of 36.3˚. Schnorenberg [Ref 2] used LDV data and surface and five-hole probe pressure measurements to study the effects of Reynolds number on the separation region at β_1= 38˚. Grove [Ref 3] experimentally and numerically investigated the flow at the

1

off-design inlet flow angle of 39.5˚ using LDV, surface and rake probe measurements and flow visualization. Nicholls [Ref 4] used the same equipment as Schnorenberg and performed tunnel calibration following the change out of the primary motor. Carlson [Ref 5] used five-hole probe, LDV and CFD data to examine end wall flow. Caruso [Ref 6] measured 3-D effects of corner vertices at β_1= 40˚ using a three component LDV system.

In 2004, Fitzgerald [Ref 7] investigated the blades at stall using a 2-D laser doppler velocimetery (LDV) system. He performed inlet, boundary layer, and wake surveys at a Reynolds number based on chord length (Re_c) of approximately 640,000. However, due to equipment operational limitations, continuous surveys were not possible, thus Fitzgerald manually reconfigured his survey equipment in order to complete his data collection.

B.   PURPOSE

The primary purpose of this study was to troubleshoot the equipment and to perform continuous LDV surveys at $Re_c \approx$ 640,000 with the blades at stall. The secondary purpose was to measure inlet conditions and take wake surveys at stall over a range of Re_c from 250,000 to 700,000. The final purpose was to perform initial numerical simulations using ESI's CFD software suite consisting of CFD GEOM, CFD ACE, and CFD View to compare computational and experimental data at both the design inlet flow angle, and the stalled condition.

II. APPARATUS AND INSTRUMENTATION

A. LOW-SPEED CASCADE WIND TUNNEL

The study was conducted in the Naval Postgraduate School's (NPS) Turbopropulsion Laboratory using the Low-Speed Cascade Wind Tunnel (LSCWT). Figure 1 depicts the layout of the NPS wind tunnel facility. Tunnel specifications are described by Nicholls [Ref 4].
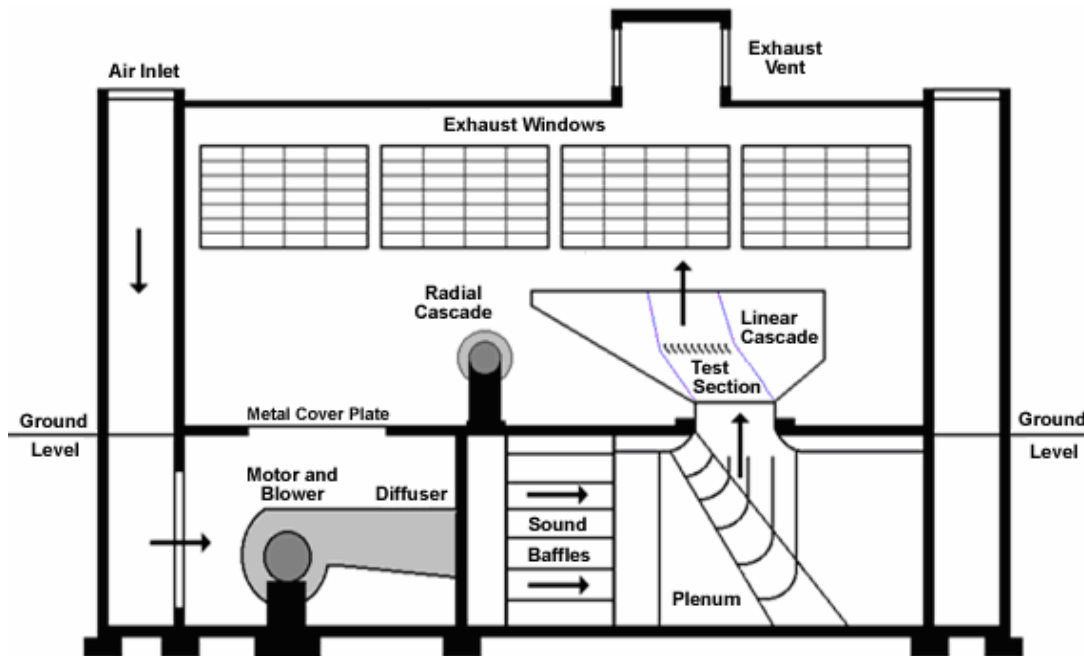
Figure 1. NPS Low Speed Cascade Wind Tunnel Facility [From Ref 7]

B. TEST SECTION

The test section of the LSCWT consisted of 10 Stator 67B controlled-diffusion (CD) blades. The installation of the blades was documented by Hansen [Ref 1]; however, as mentioned earlier the inlet flow angle, β_1, was adjusted to 40.8˚. A detailed layout of the cascade and the test section is displayed in Figure 2, and Figure 3 showed the actual blades installed. The LDV data was collected at the

3

inlet and wakes of Blades 3 and 4, and inside the boundary layer along the suction side of Blade 3. In order to facilitate LDV data collection, Blade 3 was anodized black. Blade 6 was the fully instrumented blade with 42 pressure taps used for the blade surface pressure measurements. A profile view of the 67B blades is shown in Figure 4.

Figure 2. LSCWT Test Section Schematic [After Ref 1]

Figure 3.   CD Blades Mounted in LSCWT [From Ref 7]
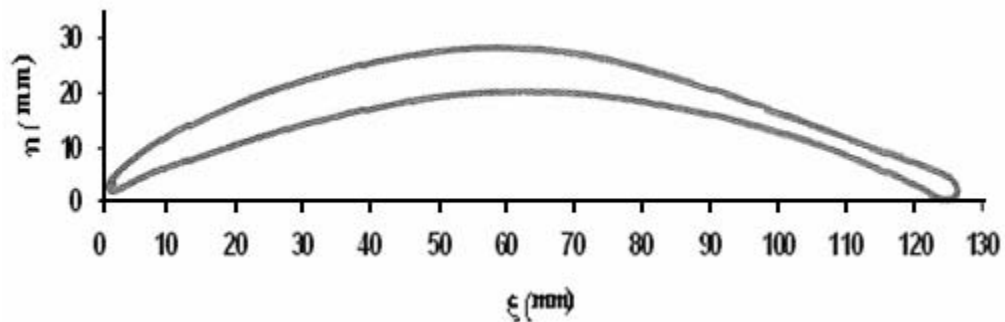
Figure 4.   Stator 67B Blade Profile [From Ref 1]

C.   INSTRUMENTATION

1.   Pressure Surveys

Surface pressure measurement data were collected from the fully instrumented Blade 6.   This particular blade included 40 pressure ports, one at each of the leading (LE) and trailing edges (TE), and 18 along the pressure side and 20 along the suction side.   Pressure port spacing is described in Lim [Ref 8].   Blade 6 was connected to a 48 channel Scanivalve system that recorded the data and that was controlled by an HP-VXI data acquisition system.   The details of the pressure data system were described by Nicholls [Ref 4].

5

2.   Laser-Doppler Velocimeter

The LDV measurement equipment used was a 3-component system built by TSI. The LDV system major subsystems of laser and optics, data acquisition and traverse mechanism were described by Fitzgerald [Ref 7].

3.   Particle Seeding

An element vital to the successful operation of the LDV system was particle seeding. The TSI model Six Jet Atomizer was used with standard olive oil as the seed source. The atomizer was set at an operating pressure of 30psi and produced seed particles on the order of 1 micron. The seeding tube was connected to a manually adjustable seed probe that allowed for adequate seeding along the survey spans. The atomizer is shown in Figure 5.

Figure 5.   Six Jet Atomizer and Particle Seeding Probe [From Ref 7]

4.   Computational Fluid Dynamics

The CFD software suite utilized to perform the numerical modeling of the cascade flow consisted of the ESI suite of software; CFD-GEOM, CFD-ACE, and CFD-VIEW. CFD-GEOM allowed the user to define the flow geometry and grid refinement. CFD-ACE performed the calculations using a pressure correction algorithm based on the SIMPLE algorithm. CFD-ACE modeled flow over both stationary and rotating objects through the choice of selecting fixed, cyclic, or rotational boundary conditions. CFD-ACE had 10 built in turbulence models that were designed for incompressible flow calculations.

THIS PAGE INTENTIONALLY LEFT BLANK

III. EXPERIMENTAL PROCEDURES

A. PRESSURE MEASUREMENTS

Pressure measurement data were collected around Blade 6 for seven test cases ranging from LSCWT plenum pressures of 2″ H_2O to 14″ H_2O, in 2″ H_2O increments. The primary plenum pressure for the research was at 12″ as this was the primary setting tested by Fitzgerald [Ref 7]. The collected data were transferred to a personal computer (PC) to be processed.

B. LASER-DOPPLER VELOCIMETRY

While the LDV system was capable of 3-D measurements, only one component had enough power to collect data. Figure 6 shows the main components and configuration of the LDV system. In order to facilitate 2-D data collection, separate surveys had to be completed at each station along the blade. First, the vertical component was measured with the green beam aligned in the standard vertical alignment position. Upon completion of the vertical survey, the fiberoptic cables leading out from the Colorburst to the fiberoptic probes for the green and blue beams were interchanged. Thus, the green beams were now in the horizontal configuration to allow for horizontal velocity component measurement.

1. Laser Calibration and Probe Alignment

At the beginning phase of research, the Argon Ion Laser system was fully cleaned and aligned following factory instruction manuals. The probe was yawed to ensure that the beam crossing was perpendicular to the LSCWT. A laser alignment tool was inserted between Blades 3 and 4 prior to each day's testing to ensure a common reference

grid. The exact specifications of the alignment tool and reference grid were found in Hansen [Ref 1]. Inlet and wake surveys were aligned with the probe perpendicular to the tunnel. Boundary layer surveys were conducted with the probe yawed 4 degrees so that the leftmost horizontal beam was aligned perpendicular to the tunnel.
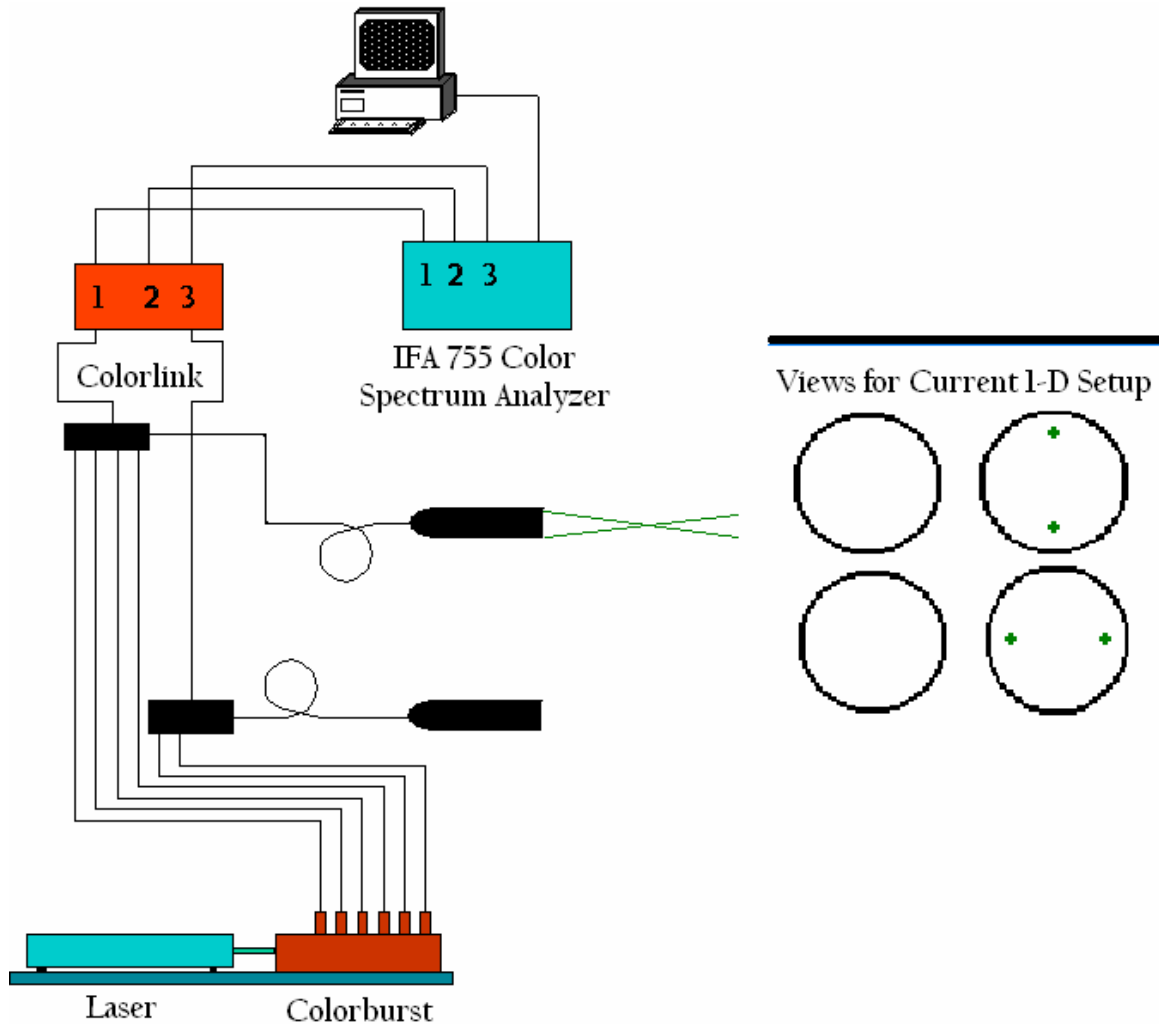
Figure 6. 1-D LDV System Configuration

2. Tunnel Calibration

In order to determine the characteristics of the LSCWT, a tunnel calibration procedure process was

10

conducted. The calibration process consisted of collecting inlet velocity data at three pressure settings, while recording the actual plenum pressure, ambient temperature, and atmospheric pressure. The recorded pressure settings were 2″ H_2O, 8″ H_2O, and 14″ H_2O of plenum pressure which were the lowest, median, and highest tunnel settings tested in this research. Pressure values for two intermediate pressure settings were then calculated via linear interpolation, giving a total of five data sets. The data was fed into a FORTRAN computer code named "Calib1.for" which provided a reference velocity for each plenum pressure setting. During each subsequent LDV survey the plenum pressure, temperature and atmospheric pressure were recorded and entered into a data file "Refer.dat." The program "Calib.1" then provided the reference velocity for each individual survey, which allowed the velocity data to be non-dimensionalized.

   3.   **Surveys**

Three types of surveys were conducted: inlet, boundary layer and wake. As previously mentioned, the main goal was to perform initial measurements at $Re_c \approx 640,000$, and all surveys were completed with the the actual value of $Re_c \approx 667,000$. Figure 7 gives the locations of the survey positions with respect to blade chord length. Velocity and turbulence intensity percentage data were collected during each survey. Using "Find" software, the survey starting Colorlink Frequency Shift and Processor Control Frequency filter settings were adjusted to conduct the surveys. A complete table of survey start settings can be found in Appendix A. The "Find" software had to be reinstalled two times in order to facilitate accurate data collection.
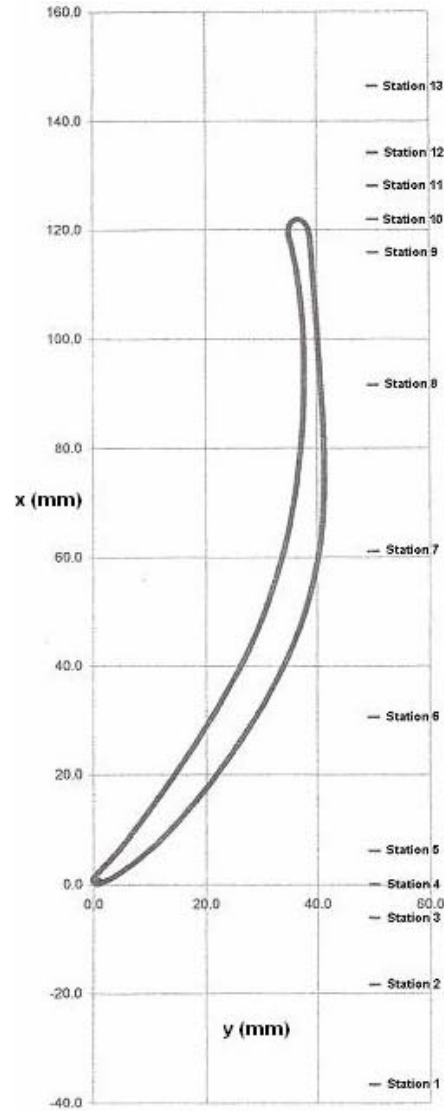
Figure 7. Laser-Doppler Survey Locations [From Ref 7]

a.   Inlet Surveys

Inlet surveys were conducted at Station 1.   A series of 25 data points which spanned 154.2 mm, equal to the blade spacing, were collected.   Station 1 was positioned 36.6 mm below the LE.   The fiberoptic probes were aligned perpendicular to the tunnel for all inlet surveys.

12

b. Boundary Layer Surveys

Although Fitzgerald performed seven boundary layer surveys, only three boundary layer surveys were conducted. Stations prior to Station 7, near mid chord, were omitted as previous data indicated that separation occurred between Stations 7 and 8. Using only the vertical beams, tangential velocity component data were collected along the blade surface. The fiberoptic probe had to be yawed 4 degrees which allowed for the beams to pass as close to the blade surface as possible.

c. Wake Surveys

At the $Re_c \approx 667,000$ tunnel setting, both coarse and fine wake measurements were conducted. Coarse surveys consisted of 50 data points collected at 5 mm intervals and passed through the wakes of Blades 3 and 4. Fine surveys performed in the wake of Blade 3 only contained 40 points at 2.5 mm spacing. Fine wake surveys were performed at $Re_c \approx 268,000$ and $Re_c \approx 545,000$. The probe was aligned perpendicular to the tunnel for all wake surveys.

THIS PAGE INTENTIONALLY LEFT BLANK

IV. NUMERICAL (CFD) PROCEDURES

COMPUTATIONAL FLUID DYNAMICS

A series of 2-D calculations were performed for the design $\beta_1 = 36.3°$ and the stalled conditions with $\beta_1 = 40.8°$. The goal was to compare results generated with the Standard k-ε, Low Re k-ε, and the k-ω turbulence models embedded in CFD-ACE with experimental data.

The mesh grid developed for the study consisted of 28,000 nodes and was designed to flow between the pressure side of one blade and suction side of the adjacent blade. One hundred grid points were placed between the blades, with a spacing of 1.542 mm between points. A total of 280 grid points defined the flow path from the inlet to the outlet. The grid geometry is shown as Figure 8.

The design point calculations consisted of 100 iterations for each turbulence model. The number was chosen so that at least three orders of magnitude convergence were achieved on the residuals.
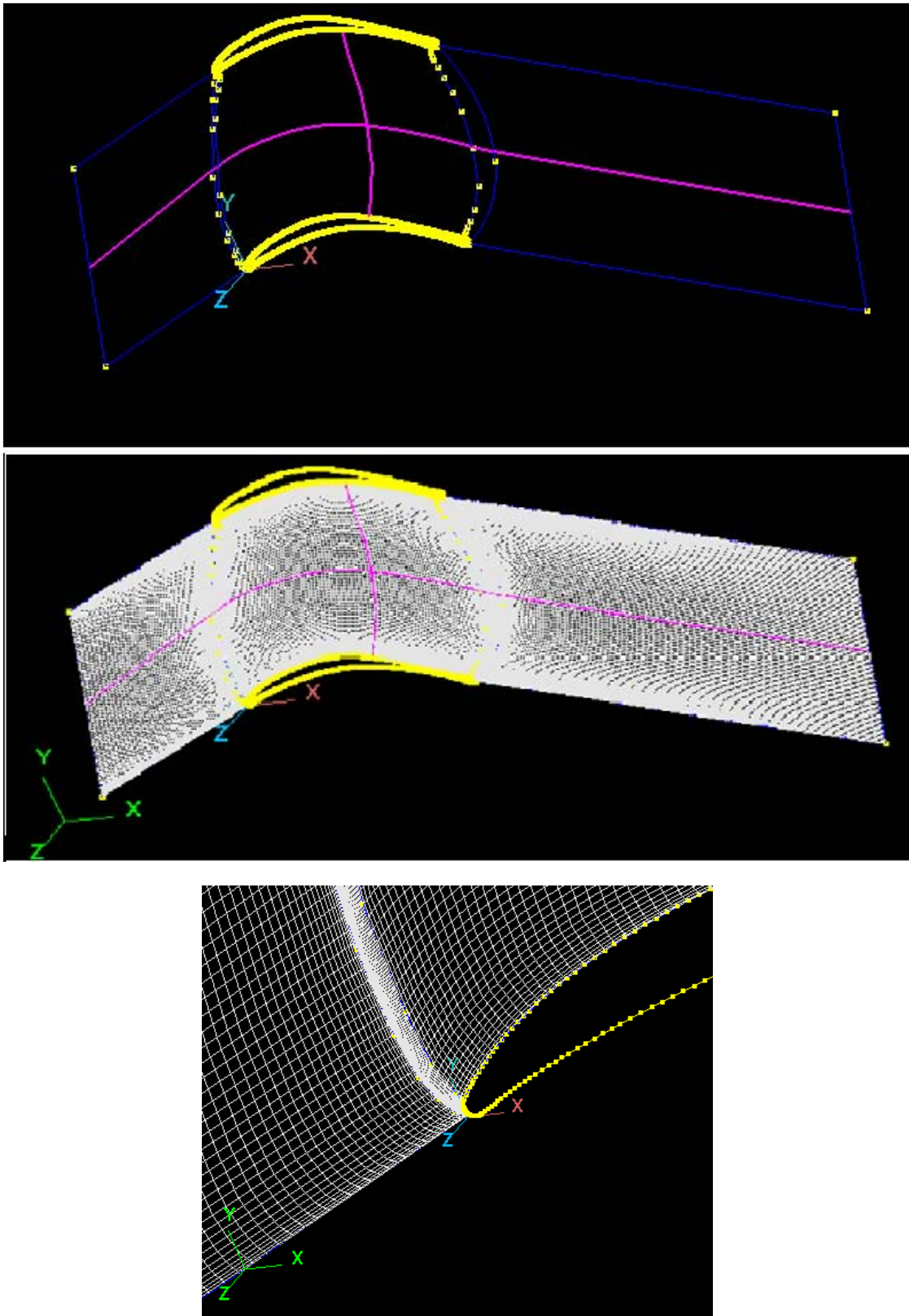
Figure 8.   Mesh Grid Geometry With Close Up of Leading Edge

V. RESULTS AND DISCUSSION

A. PRESSURE SURVEYS

Blade surface pressure measurements taken on Blade 6 verified that the blades were indeed at stall. Figure 9 shows Cp vs x/c for the highest, lowest and median tunnel settings plotted against one another. At $Re_c \approx 268,000$, at approximately x/c = 0.43 a leveling off of the Cp along the suction side of the blade indicated that the flow separated and then reattached at x/c = 0.7. As Rec increased to 545,000, there was no evidence that the flow reattached on the blade surface, thus showing the stalled condition. Notably, as Rec increased, the enclosed area between the suction side and pressure side Cp distributions decreased, which resulted in a loss of lift. Cp plots for each of the 7 tunnel plenum pressure conditions were included in Appendix B.
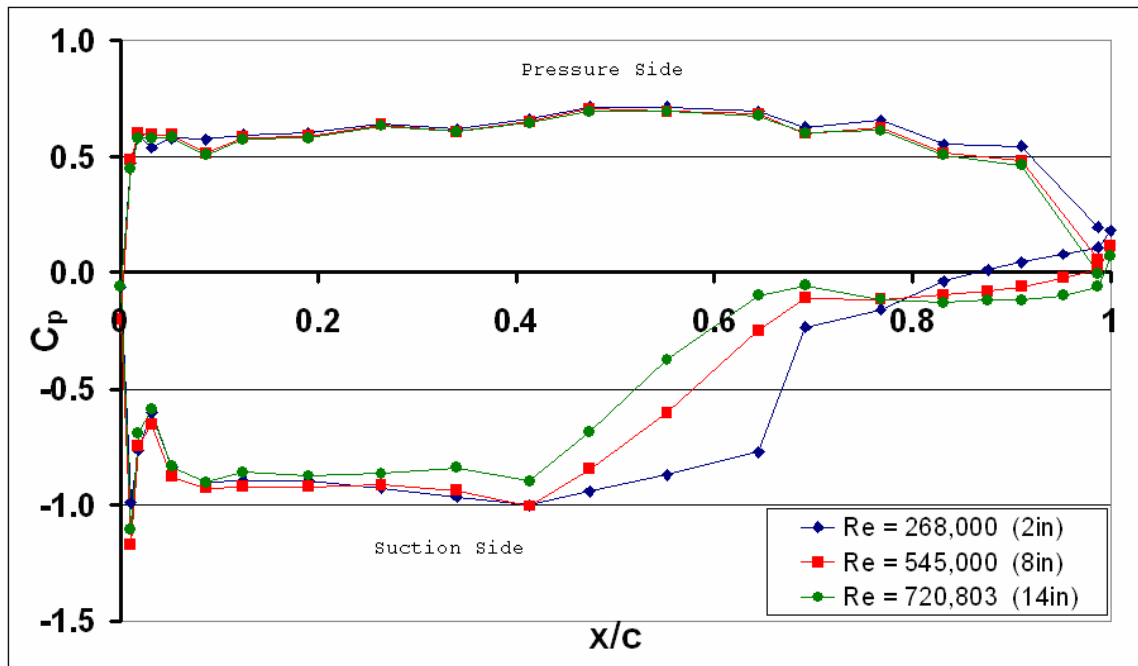
Figure 9. Pressure Ratio Distributions at Various Re_c

17

B. LASER-DOPPLER VELOCIMETRY AT $RE_C \approx 667,000$

    1. Inlet Surveys

       The results of inlet surveys are displayed in Figure 10. As $\beta_1 = 40.8°$, the horizontal and vertical velocity components were nearly equal. The flow demonstrated a mild sinusoidal velocity nature which was a result of the potential effect of the leading edges of Blades 3 and 4 felt upstream. Average turbulence intensity (TI%) for the vertical component was 1.6% and for the horizontal component 1.7%.
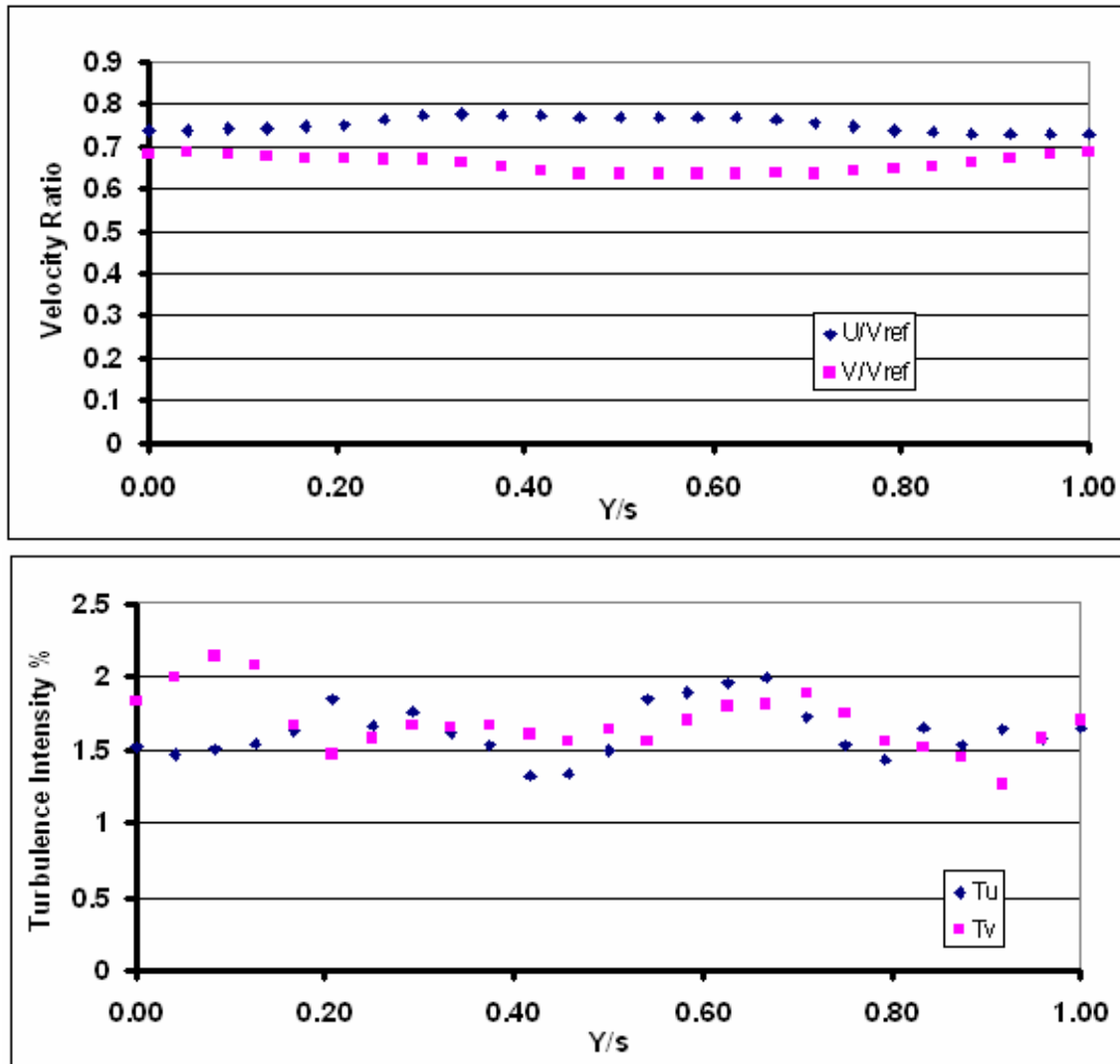
Figure 10.   Station 1 Inlet Survey @ $Re_C \approx 667,000$

2. Boundary Layer Surveys

Boundary layer surveys were only conducted at a $Re_c \approx$ 667,000, to ensure verification of Fitzgerald's thesis work [Ref 8]. Three boundary layer surveys were collected at Stations 7, 8, and 9 respectively. As mentioned previously, the LDV probe was yawed 4 degrees to allow for the beam crossing to reach as close to the blade surface as possible, and the horizontal component could not be measured due to blade camber.

a. Station 7 Boundary Layer Survey

Figure 11 contains the graphical output of the survey at Station 7. The freestream velocity remained relatively unaffected until very near the blade surface. The value of d/c was a ratio of the distance from the blade surface vs chordlength, and a value of d/c = 0.05 was approximately 6.4 mm away from the blade surface. The flow velocity remained positive, and thus validated Fitzgerald's observation that separation occurred downstream of Station 7. Turbulence intensity remained steady at 4% in the freestream until it reached d/c of 0.10, and then increased to a maximum of 12% as d/c went to zero.

b. Station 8 Boundary Layer Survey

Station 8 can be seen in Figure 12. The boundary layer at this station was measured to extend away from the blade by a normalized distance (d/c) of 0.15, or 12.8 mm from the blade surface. At d/c of 0.05, the flow became negative and demonstrated that separation had occurred and that there was a region of reverse flow present. Again, this showed agreement with Fitzgerald's data. Turbulence intensity began increasing above 4% at d/c =0.4 and had two peaks. The first peak showed a turbulence intensity of 18%

19

at d/c = 0.13 at the point of maximum shear in the positive flow.   The second, higher peak at d/c = 0.06 reached over 20% and showed the maximum shear in the reverse region.
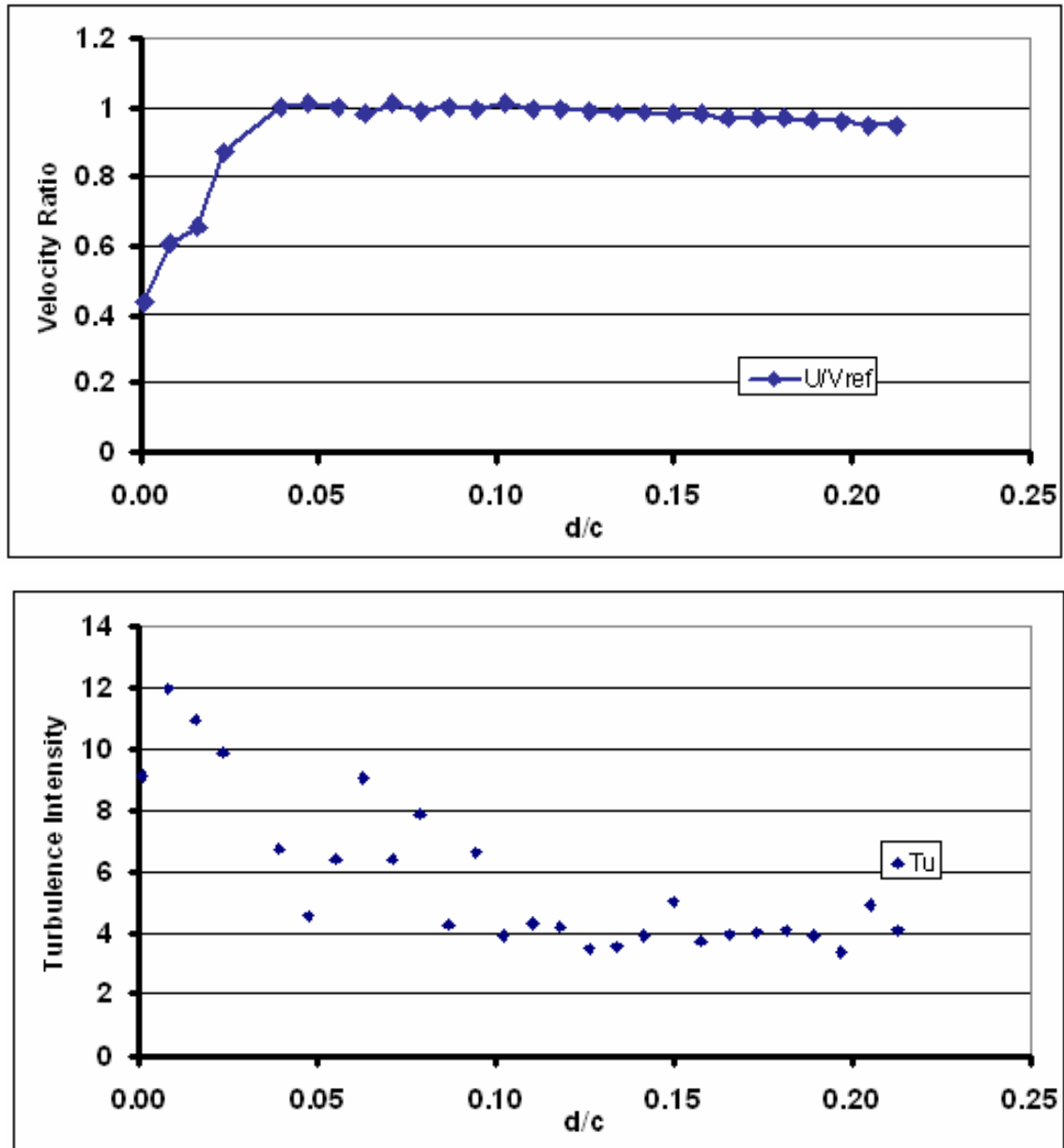
Figure 11.   Station 7 Boundary Layer Survey @ $Re_c \approx 667,000$
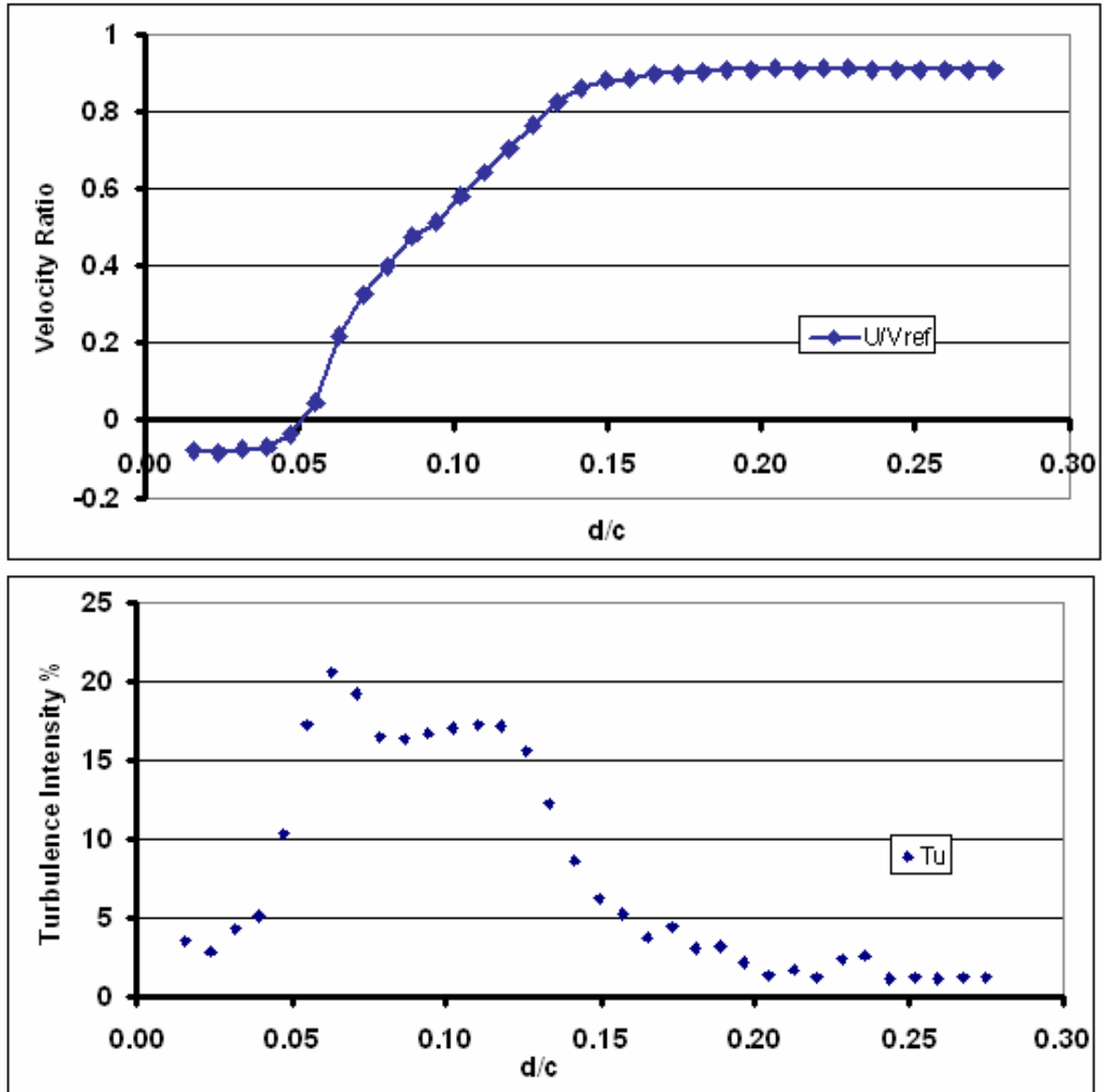
Figure 12.   Station 8 Boundary Layer Survey @ Re_c ≈ 667,000

c.   Station 9 Boundary Layer Survey

Station 9 data can be seen in Figure 13.   As expected, the freestream velocity became affected further from the blade surface at d/c = 0.25.   The region of reverse flow grew to twice the size of that at Station 8, which was consistent with previous measurements [Ref 6]. Two peaks in turbulence intensity were measured, with the first seen at the location where the flow returned to

21

freestream conditions, and the second higher peak at the point where the flow became reversed. The turbulence intensity percentages were 18% and 21% for the two cases respectively.

3.   Wake Surveys

Wake Surveys were completed at Stations 11, 12, and 13. The probe was aligned perpendicular to the tunnel for all surveys, and horizontal and vertical components of the flow were measured.

a.   Station 11

The graphical outputs of the surveys at Station 11 are shown as Figure 14 and include the velocity ratios for both the coarse and fine surveys as well as the turbulence intensity of the coarse survey. In the wake of Blade 3 and 4 a region of reverse flow was measured in the horizontal and vertical flow components. The fine survey indicated that the width of the reverse flow region was on the order of 13 mm, which spanned from Y/s = 0.25 to 0.32 behind Blade 3. The turbulence intensity peaked at approximately 16% at the location where the flow reverted back to freestream conditions. Turbulence intensity was 2.2% in the freestream, very near to the original inlet conditions.
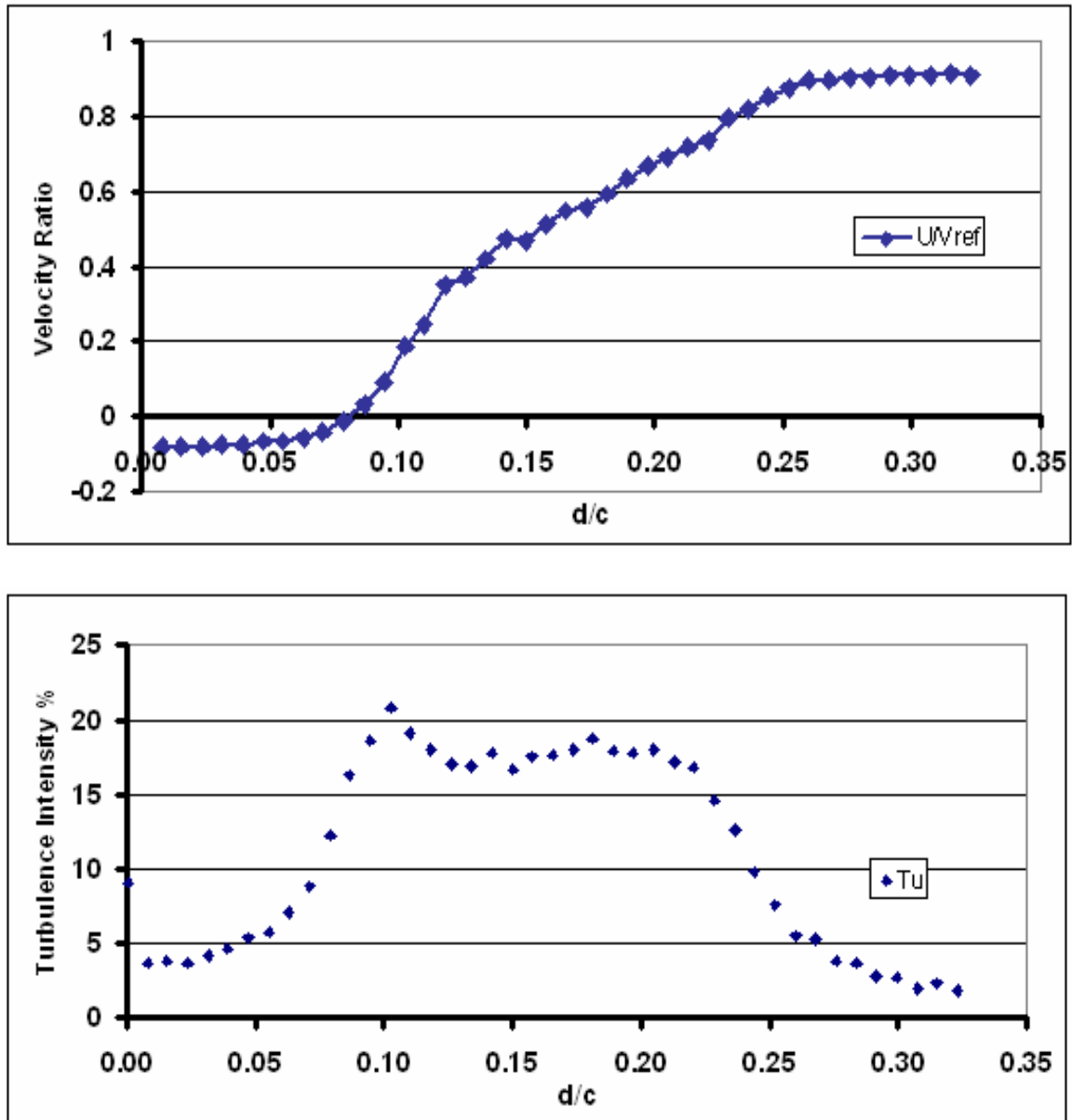
Figure 13.   Station 9 Boundary Layer Survey @ $Re_c \approx 667,000$
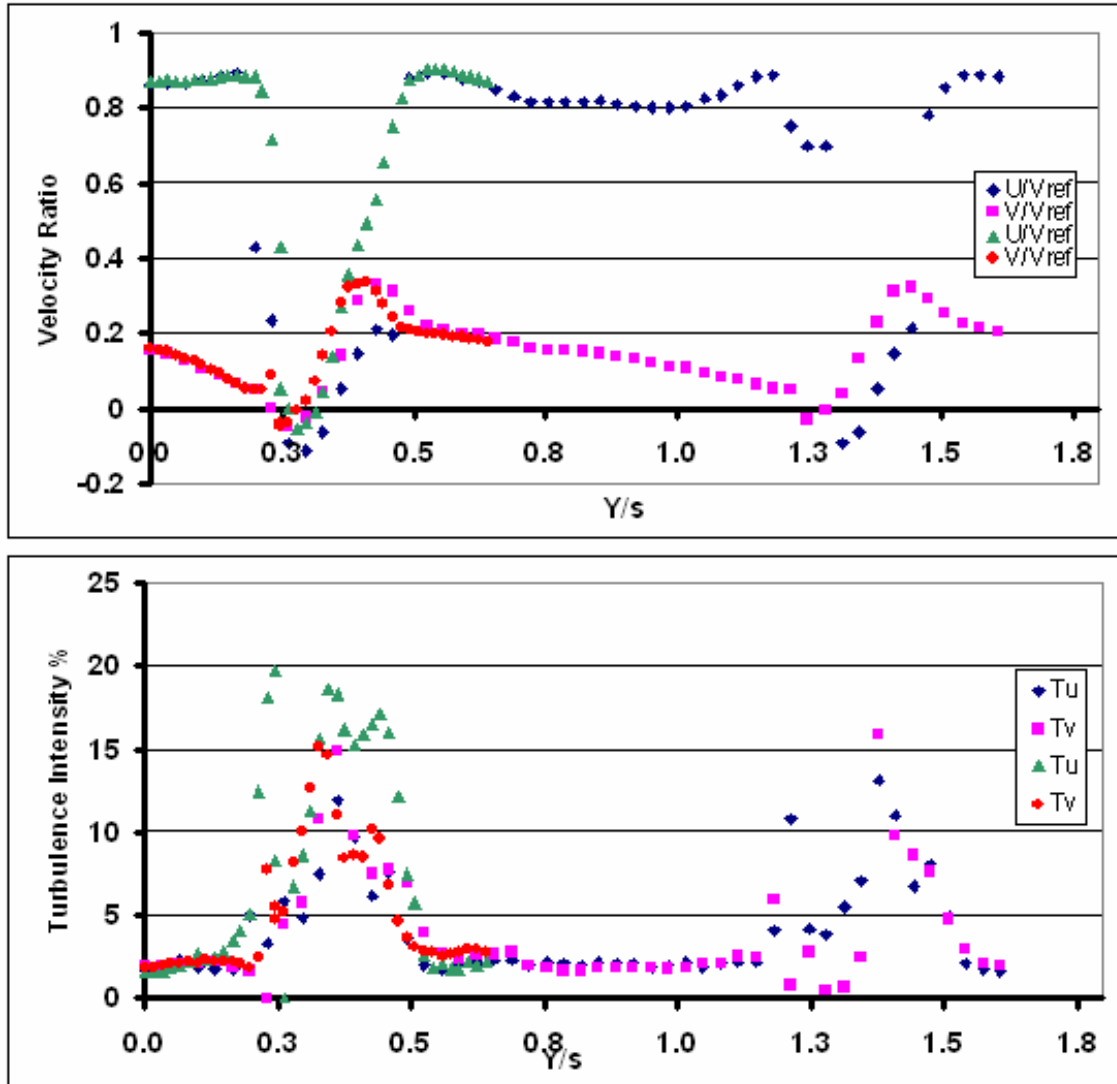
Figure 14.   Station 11 Wake Survey @ $Re_c \approx 667,000$

b.   Station 12

Station 12 again showed reverse flow in the horizontal and vertical flow components, as seen in Figure 15.   In the wake of Blade 3, the reverse flow region decreased in size and spanned from Y/s = 0.28 to 0.31, as seen in the fine survey plot.   The turbulence intensity recorded for the coarse survey in the wake spiked above 20% Tu. These points correspond to regions of maximum shear in the mean flow.   The data for the fine survey at Station 12

were included in Figure 15 and indicated that the turbulence intensity for the vertical component was consistent with Station 11 as well as Fitzgerald's data.
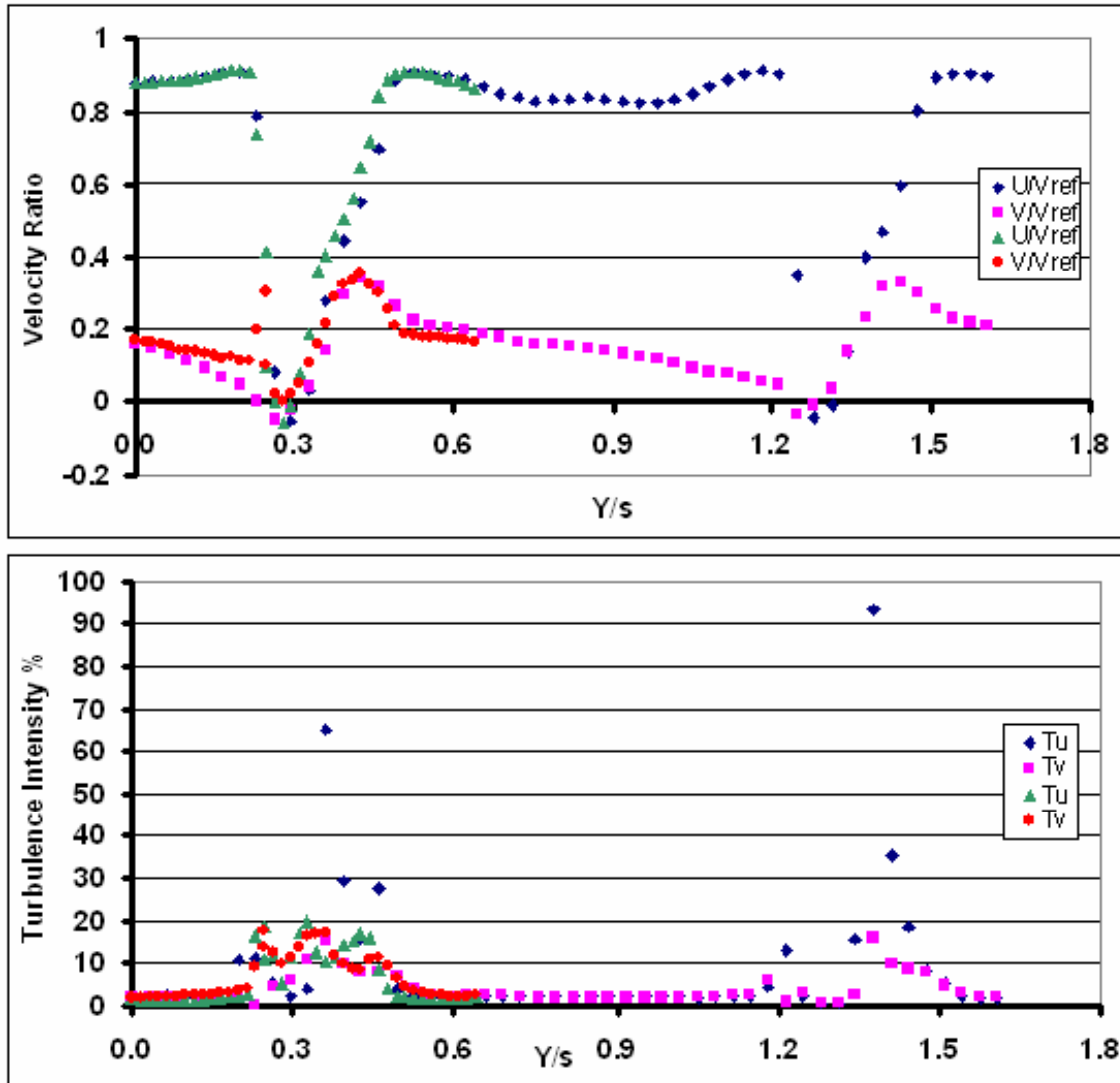
Figure 15.   Station 12 Wake Survey @ Re_c ≈ 667,000

c.   Station 13

Station 13 results, plotted in Figure 16, showed that the region of reverse flow had dissipated in the freestream. Turbulence intensity retained a very similar profile to Station 11, with peaks as high as 17% in the

wake of Blade 3 and 16% in the wake of Blade 4. The peaks occurred in the region where the freestream flow began to slow and where the affected flow returned to freestream conditions.
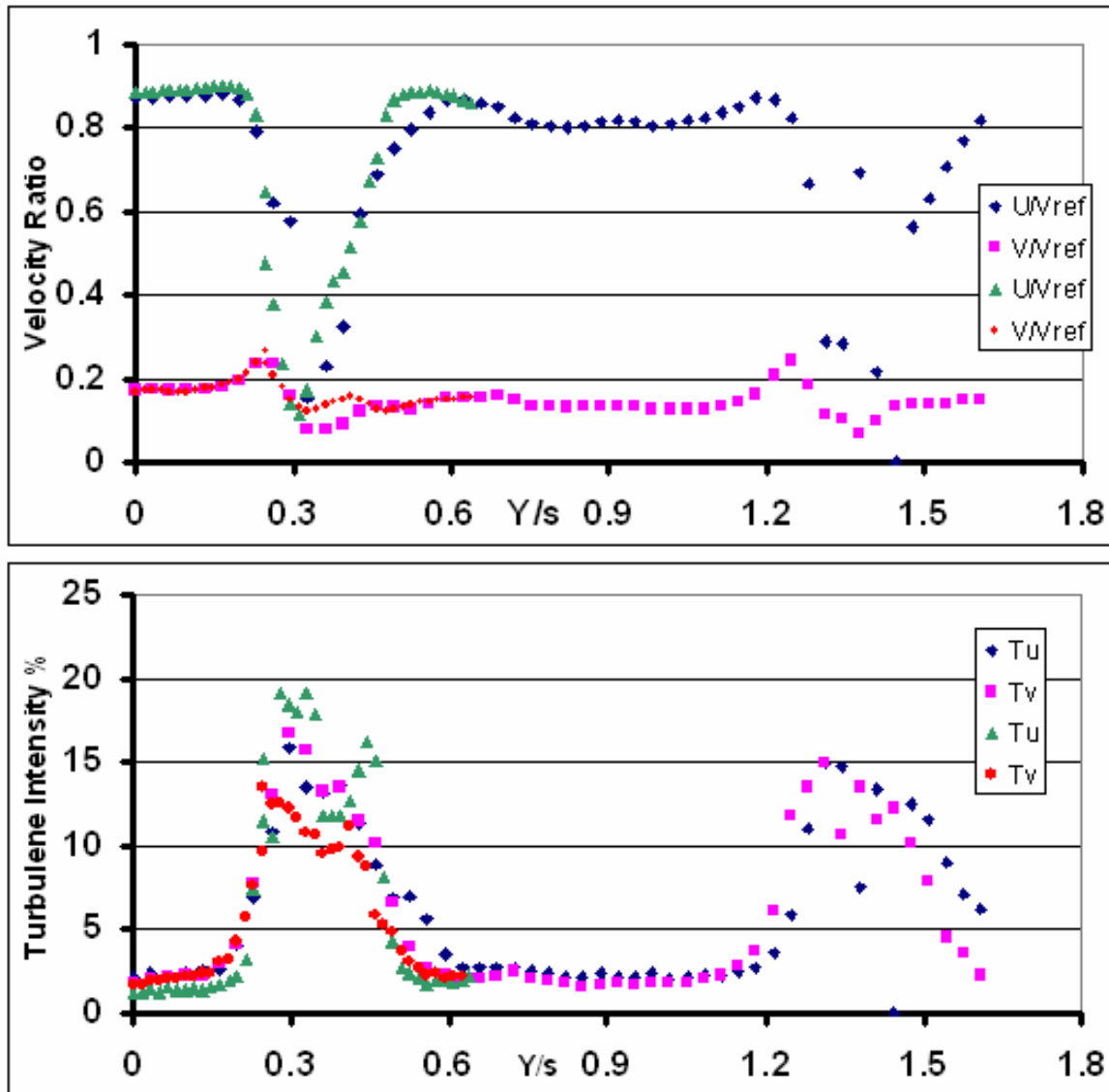
Figure 16.   Station 13 Wake Survey @ $Re_c \approx 667,000$

C.   LASER-DOPPLER VELOCIMETRY AT $RE_C \approx 268,000$

1.   Inlet Surveys at $Re_c \approx 268,000$

Inlet survey results can be found in Figure 17. The flow velocity ratios and turbulence intensity were

consistent with those collected at $Re_c \approx 667,000$. The potential from the LE of Blades 3 and 4 were viewed by the low amplitude sinusoidal pattern in the velocity ratio data. The turbulence intensity remained in the 1.5-2.0% range for both velocity components.
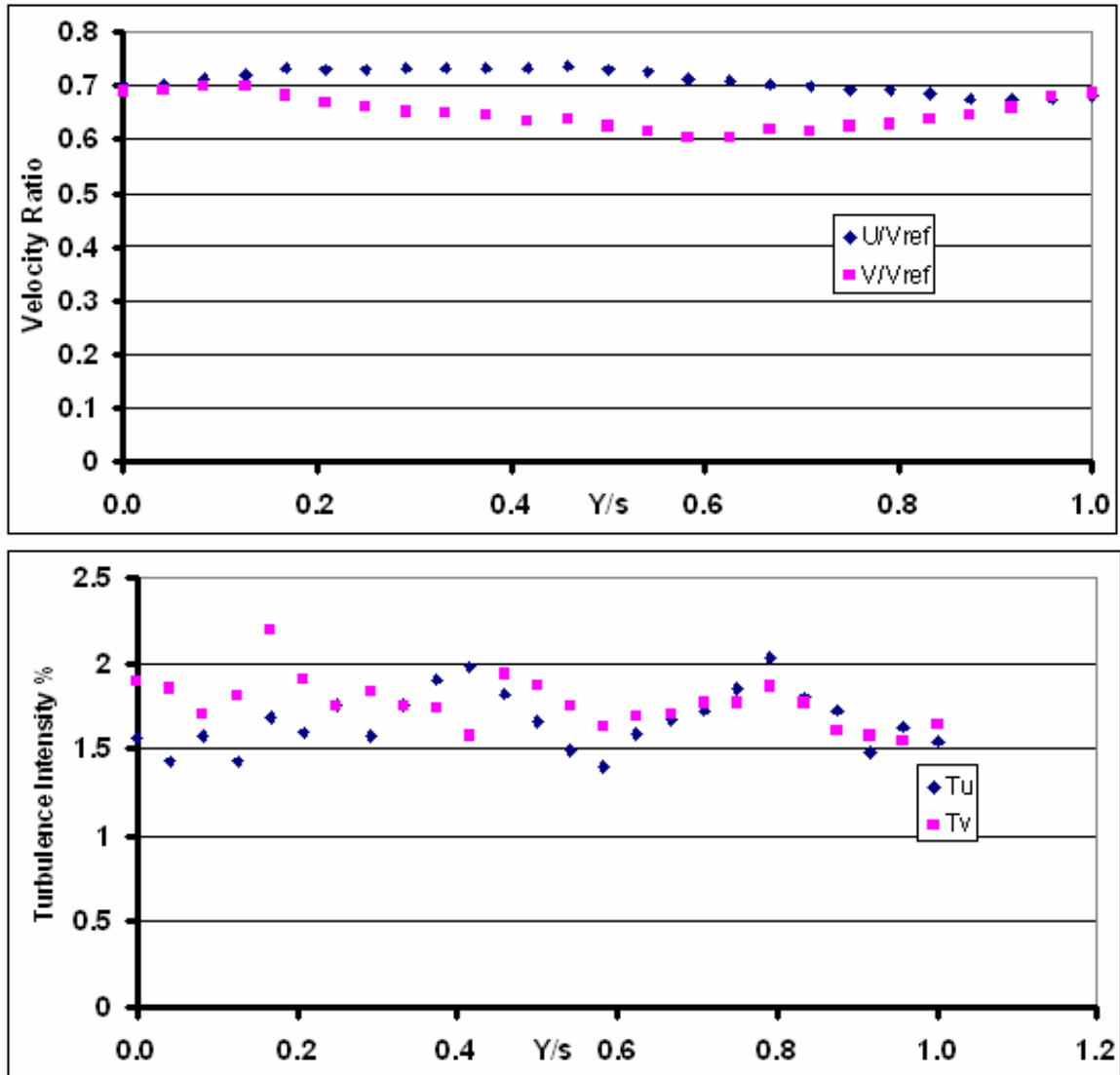
Figure 17.   Station 1 Inlet Survey @ $Re_c \approx 268,000$

27

2.   Wake Surveys at $Re_c \approx 268{,}000$

a.   *Station 11*

Station 11, plotted data shown in Figure 18, showed a very different nature than observed at $Re_c \approx 667{,}000$. The magnitudes of the velocity ratios between the two cases showed good agreement; reverse flow in the horizontal and vertical flow was measured in the wake. The vertical turbulence, Tu, reached a maximum of 42% where the flow returned to freestream conditions. While Tu was more than double that measured at $Re_c \approx 667{,}000$, Tv, or the horizontal turbulence intensity, peaked at 10% which was half that seen at the higher Re_c. The plot of Tv showed two peaks which coincided with the locations of the extreme boundaries of the reverse flow region. Tu showed a single peak at Y/s = 0.3 that coincided with the second Tv peak.

b.   *Station 12*

Station 12 flow behavior again demonstrated a region of reverse flow, although less intense than at Station 11. The Tu value measured remained higher than Tv, but a drop in Tu and rise in Tv was observed. Peak Tu dropped to 38% and peak Tv rose to 18%. Figure 19 contains the graphical output at Station 12. As at Station 11, Tu had a single peak, and Tv had double peaks.

c.   *Station 13*

Station 13 data, depicted in Figure 20, showed that the disturbed flow region was being carried away in the freestream. Neither velocity component underwent reverse flow, and the gradients in the mean velocity profile were steeper than those measured at $Re_c \approx 667{,}000$. As seen at Station 12, the Tu and Tv values converged, as Tu dropped to 26% and Tv rose to 19%. The Tu and Tv curves

also had steep slopes that matched the velocity curves. Twin peaks were measured for both Tu and Tv.
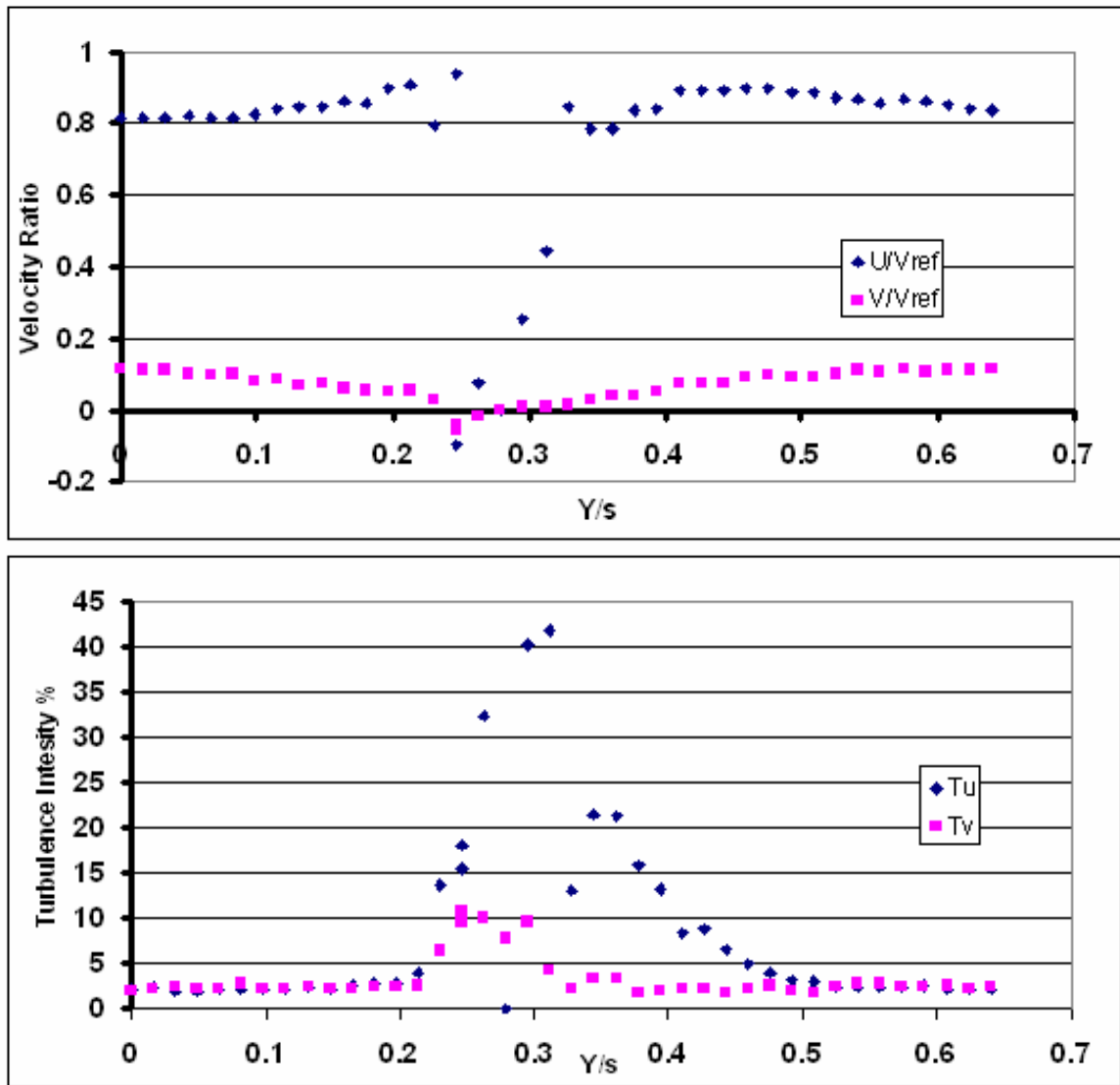
Figure 18.   Station 11 Wake Survey @ $Re_c \approx 268{,}000$
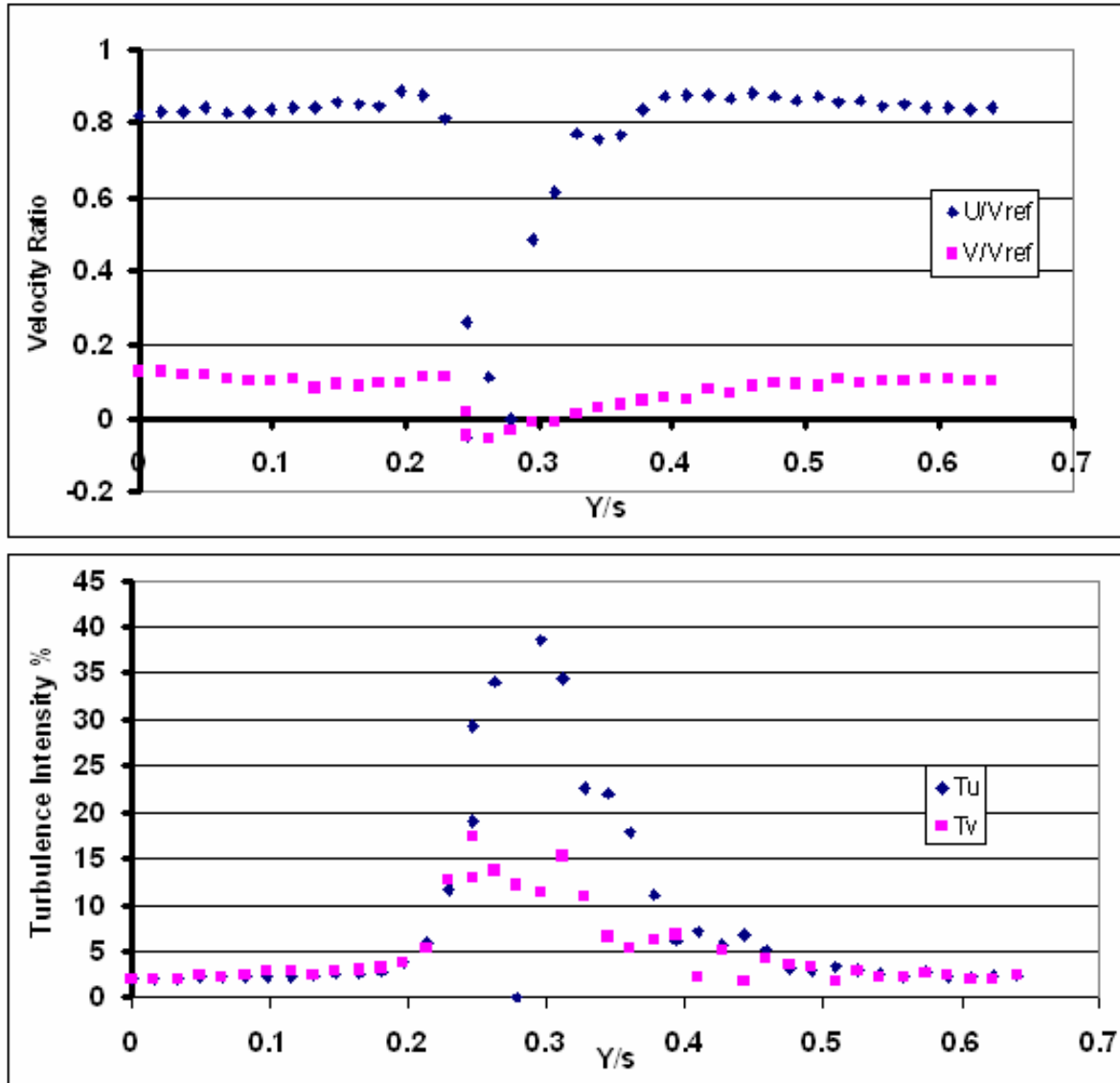
Figure 19.   Station 12 Wake Survey @ $Re_c \approx 268,000$
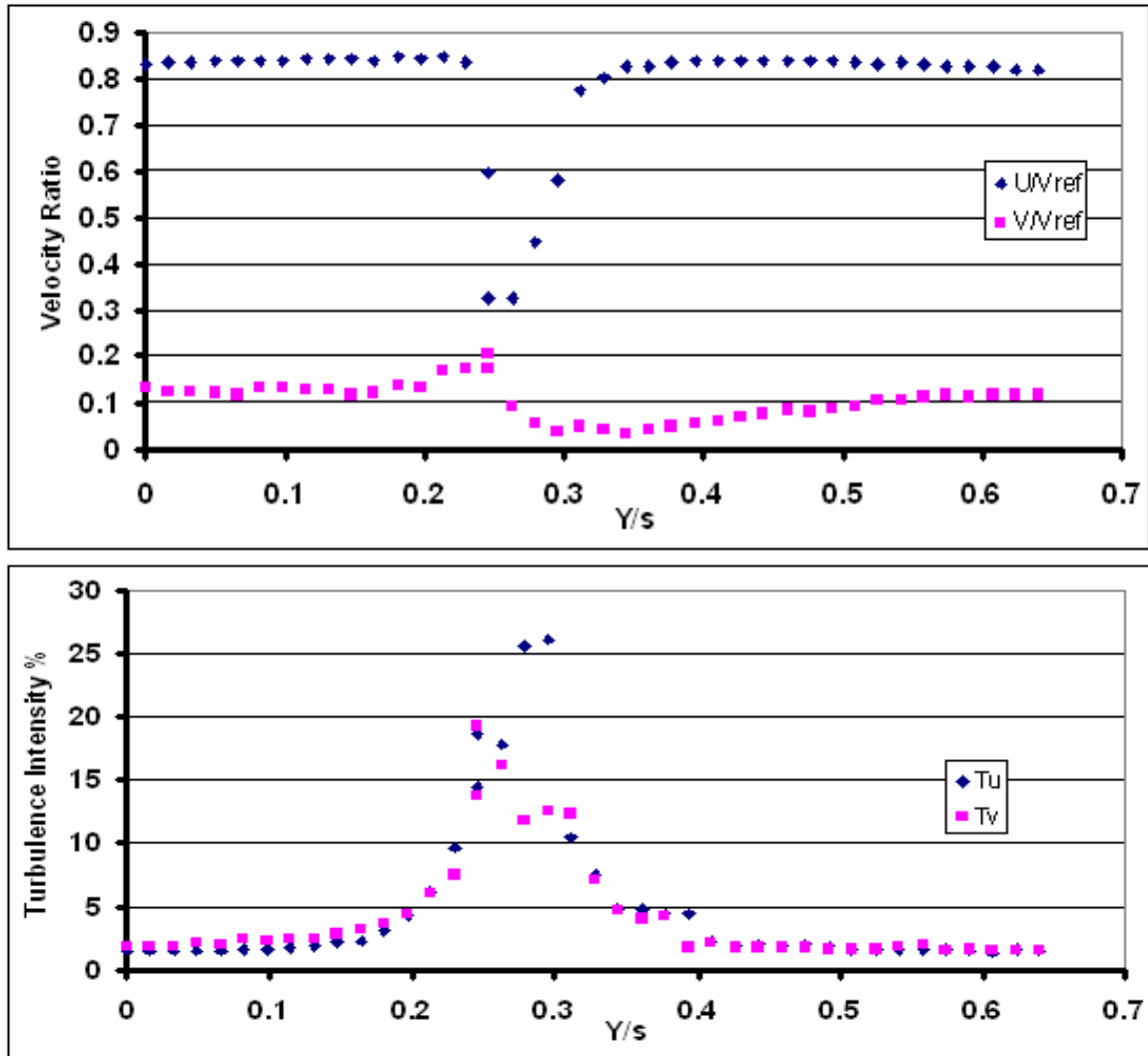
Figure 20.   Station 13 Wake Survey @ Re$_c$ ≈ 268,000

D.   LASER-DOPPLER VELOCIMETRY AT RE$_C$ ≈ 545,000

1.   Inlet Surveys

Inlet survey output is displayed as Figure 21. Velocity ratio data coincided very closely with that measured at the other two test conditions. Turbulence intensity in the vertical component was recorded as ranging from 1.5-2%, as before, but Tv had a higher average as well as higher overall total change, fluctuating between 1.9% and 2.7%.
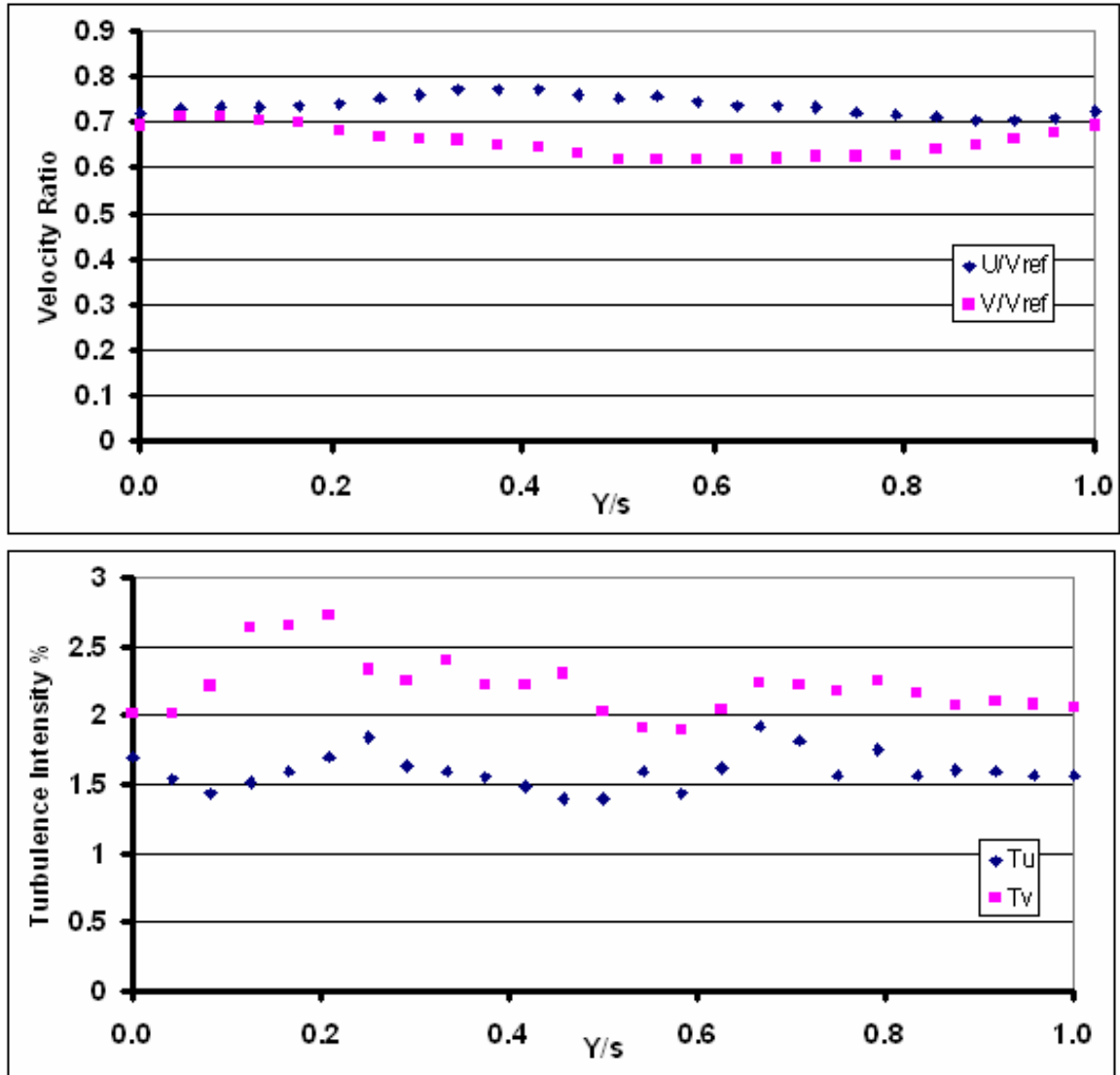
Figure 21.   Station 1 Inlet Survey @ $Re_c \approx 545,000$

2.   Wake Surveys

a.   Station 11

Station 11 showed that a reverse flow region was present for both velocity components. Refer to Figure 22 for the graphical output. While both velocities were negative, the vertical component velocity ratio was more highly negative than the horizontal. As seen at $Re_c \approx$ 268,000, Tu was higher than Tv, although at the higher Re_c

32

the difference was smaller. The turbulence intensity curves showed a very distinct nature from the other two test cases. There were two distinct peaks in Tu, as well as a plateau. The first peak of 35% at Y/s = 0.25 occurred at the beginning of the reverse flow region. The second peak of 22.5% at Y/s = 0.33 coincided with the end of the reverse flow region. Tu then dropped slightly to 18% until the flow returned to freestream conditions. There was a similar profile in Tv, but both peaks were nearly 15%.
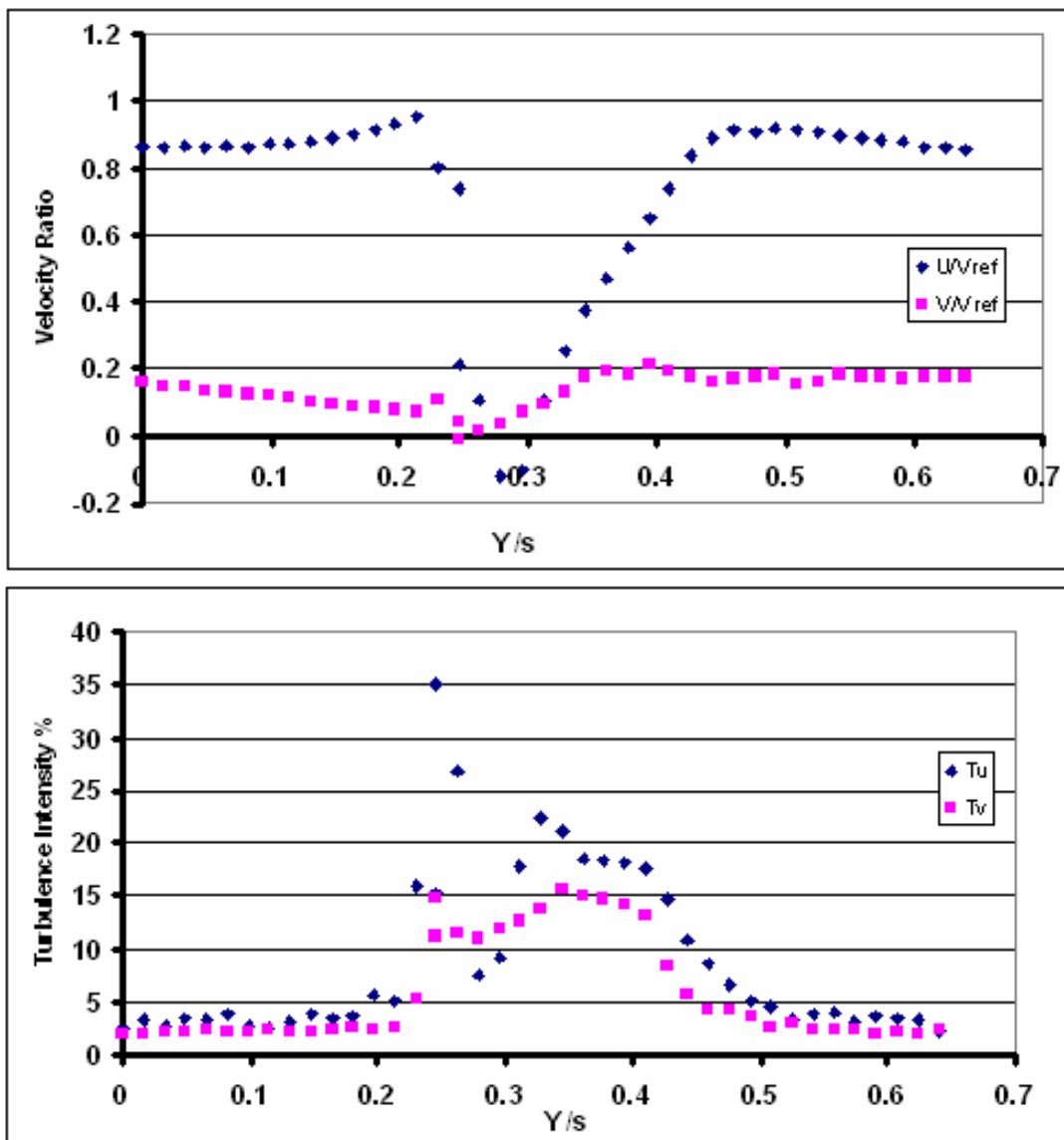
Figure 22. Station 11 Wake Survey @ Re$_c$ ≈ 545,000

b.   *Station 12*

Station 12 at $Re_c \approx$ 545,000 showed the most remarkable flow characteristics of all the Stations tested. The velocity ratio data looked much like the other wake stations, with reverse flow in the vertical component and either very slow flow or slightly reverse flow in the horizontal component.   The turbulence intensity profiles were very different than those observed at the other stations and Re_c.   In looking at the Tu and Tv plots in Figure 23, three distinct peaks were clearly seen for both turbulence intensity values.   Each component peaked at the extreme edges of the reverse flow region and at the return to freestream conditions.   Most noteworthy was the change of peak magnitudes between Stations 11 and 12.   For Tu at Station 11, the peak turbulence intensity was at the beginning of the reverse flow region, and each successive peak or plateau was at a lower value.   At Station 11 Tv showed a different profile that had its highest peak at the end of the reverse flow region.

At Station 12, Tu had its maximum value at the end of the reverse flow region rather than at the beginning, and had a similar shape, although different magnitude, as Tv at Station 11.   Tv peaked at the beginning of the reverse flow region and each successive peak was lower, much as Tu looked at Station 11.   Thus, there was a swap in the nature of how Tu and Tv behaved between Stations 11 and 12.   This was difficult to explain in 2-D terms, but it indicated that the flow region was highly 3-dimensional and complex in nature.
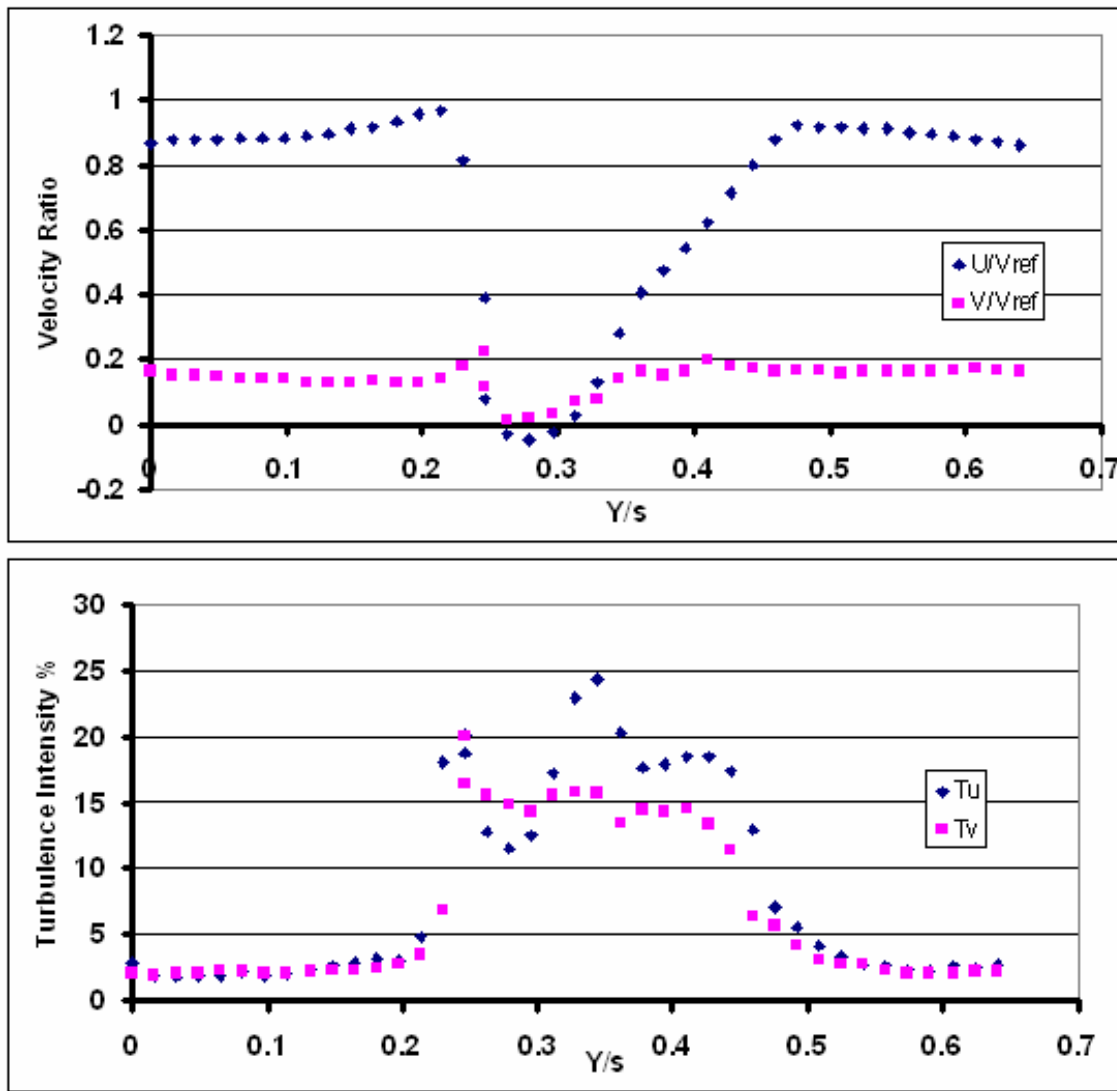
Figure 23.   Station 12 Wake Survey @ $Re_c \approx$ 545,000

c.   Station 13

Station 13 data plotted in Figure 24 showed that the wake had less of a deficit as it was carried away from the trailing edge. No reverse flow was seen in either velocity component. Vertical turbulence intensity actually peaked at a higher value (28% vs 24.5%) here than at Station 12, but there was a single peak with steep slopes, which gave an overall lower average value of Tu. A similar

average value of turbulence intensity was seen for Tv, and a similar peak value, but like Tu it had the maximum turbulence more centralized around a single peak.
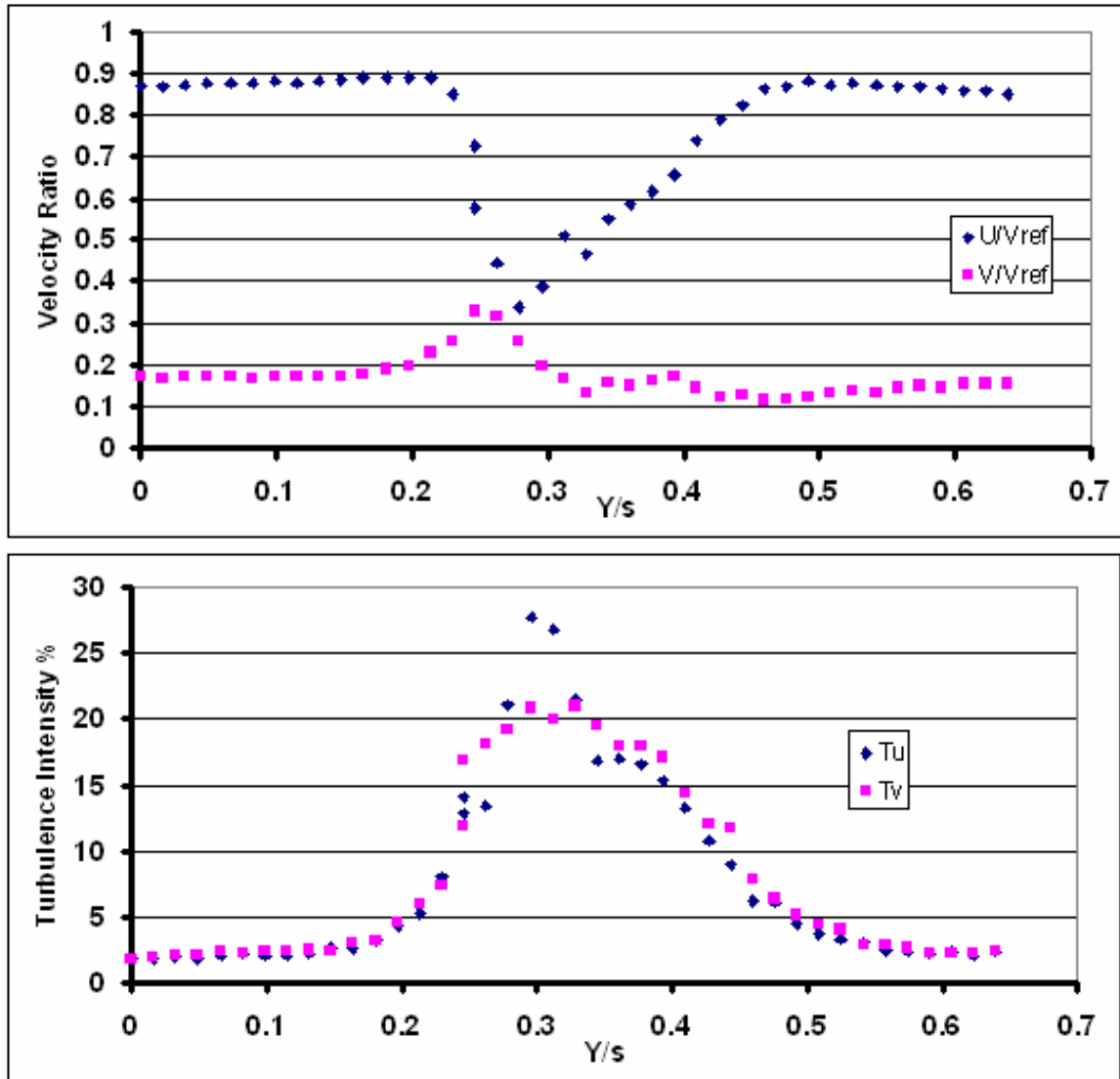
Figure 24.   Station 13 Wake Survey @ $Re_c \approx 545,000$

E.   COMPUTATIONAL FLUID DYNAMICS

   1.   Results at Design Conditions (β_1 = 36.3˚)

Both the k-ε and Low Re k-ε turbulence models gave solutions at 100 iterations; however the k-ω model trials always diverged before reaching 100 iterations. Thus no data was available for the k-ω model. The other two models' solutions also diverged before reaching 200 iterations, thus the data predicted at 100 iterations will be discussed.

Figures 25 and 26 show graphical output data from the CFD modeling effort. Figure 25 shows the pressure and velocity contour fields through a set of adjacent blades computed with the k-ε model. The fields looked appropriate, and thus Cp data were then extracted from CFD VIEW output. When the CFD data were plotted versus Hansen's experimental data [Ref 1] the data did not closely match (Figure 26). The pressure side of the blade showed better agreement than did the suction side, but from the leading edge to x/c = 0.3 along the pressure side Cp data showed poor agreement. The CFD generated Cp curve along the pressure side showed the same shape as the experimental data, but the ratio was under-predicted along the entire chord. The Standard k-ε model data was slightly closer to the actual data than the Low Re k-ε data.

Along the suction side, the CFD data again showed a similar shape to the experimental data, but again under-predicted the ratio along the entire chord. Similar to the pressure side, the worst prediction for the suction side was from the leading edge to x/c of 0.5.

37
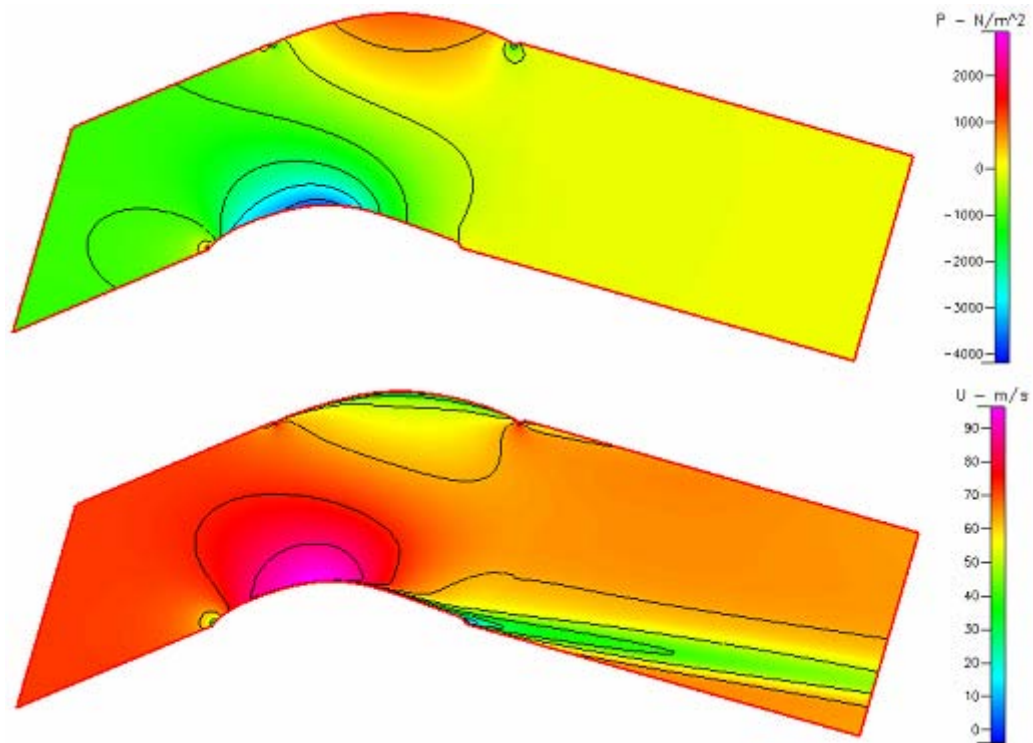
Figure 25.   Pressure and Velocity Distribution @ β_1 = 36.3°
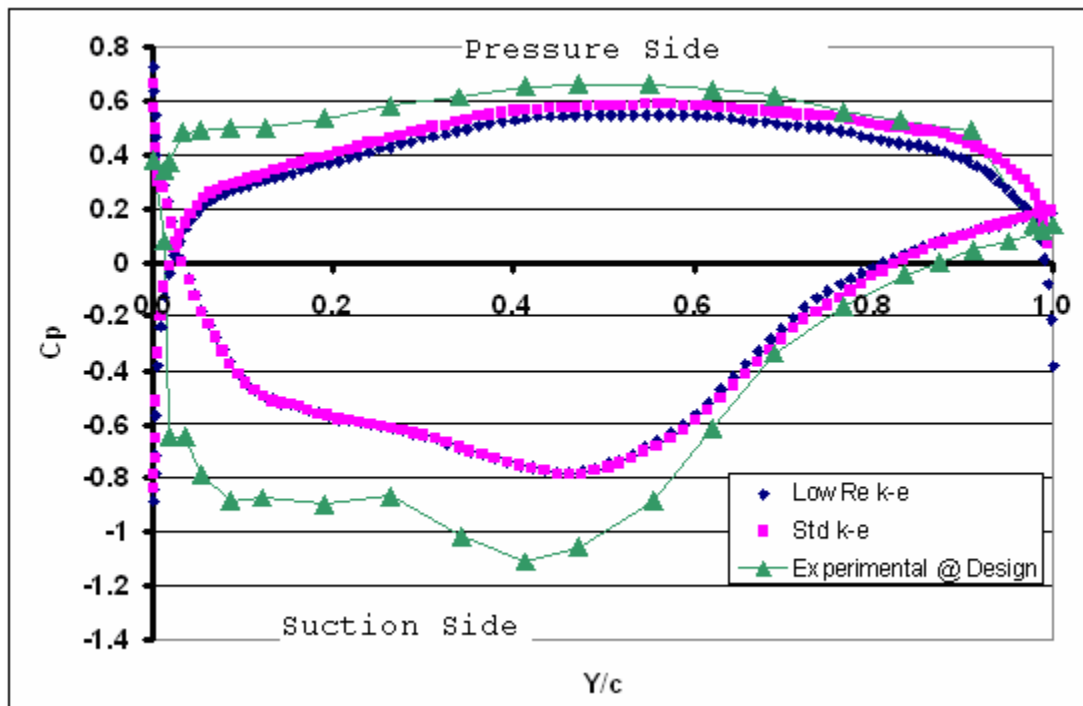
Figure 26.   CFD and Experimental Cp Distribution Comparison
at Design β_1

2.   Results at Stalled Design Conditions ($\beta_1 = 40.8°$)

In spite of the lack of agreement with the experimental at design inlet flow angle, the stall condition was also computed. As before, the k-ω solutions diverged, but the other two models gave solutions at 100 iterations, but diverged before 200 iterations could be performed successfully.

Figure 27 shows the contour plots of the pressure and velocity fields for the blade passage and both appear to offer reasonable solutions. The Cp was then extracted from VIEW and plotted against the experimental Cp data collected during the current study. The results of this comparison are plotted in Figure 28.

The results spanning the chordlength of the pressure side were very similar to the design case. Again, the CFD code failed to accurately predict the leading edge conditions. However, from x/c of 0.5 to 0.8 the results actually showed reasonable agreement with the experimental results.

As for the design β_1 comparison, there was less correlation between CFD and experimental results along the suction side of the blade for the stalled condition. The leading edge was again the least accurate portion of the CFD prediction. But, unlike the design case, the suction side solution did not under-predict the Cp distribution as it had earlier. Rather, the data lines crossed twice; first at x/c = 0.5 and again at x/c = 0.75. This was possibly the result of the limitations of a 2-D model to accurately predict a highly turbulent, separated, 3-D flow.
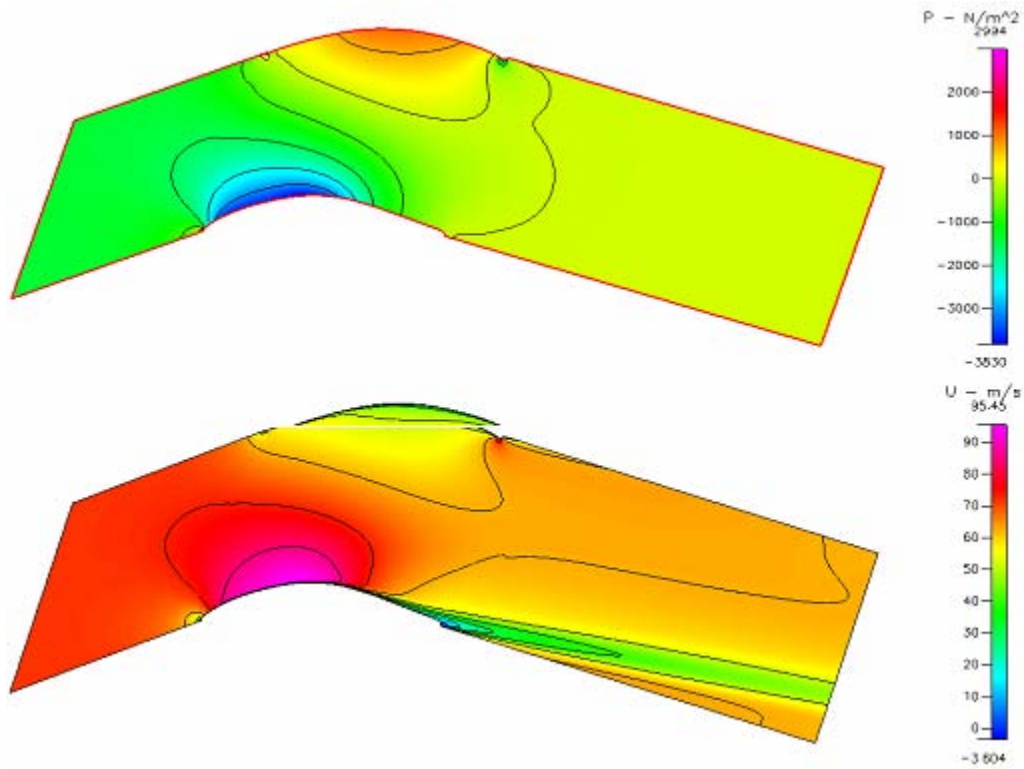
Figure 27.   Pressure and Velocity Distribution @ β_1 = 36.3˚
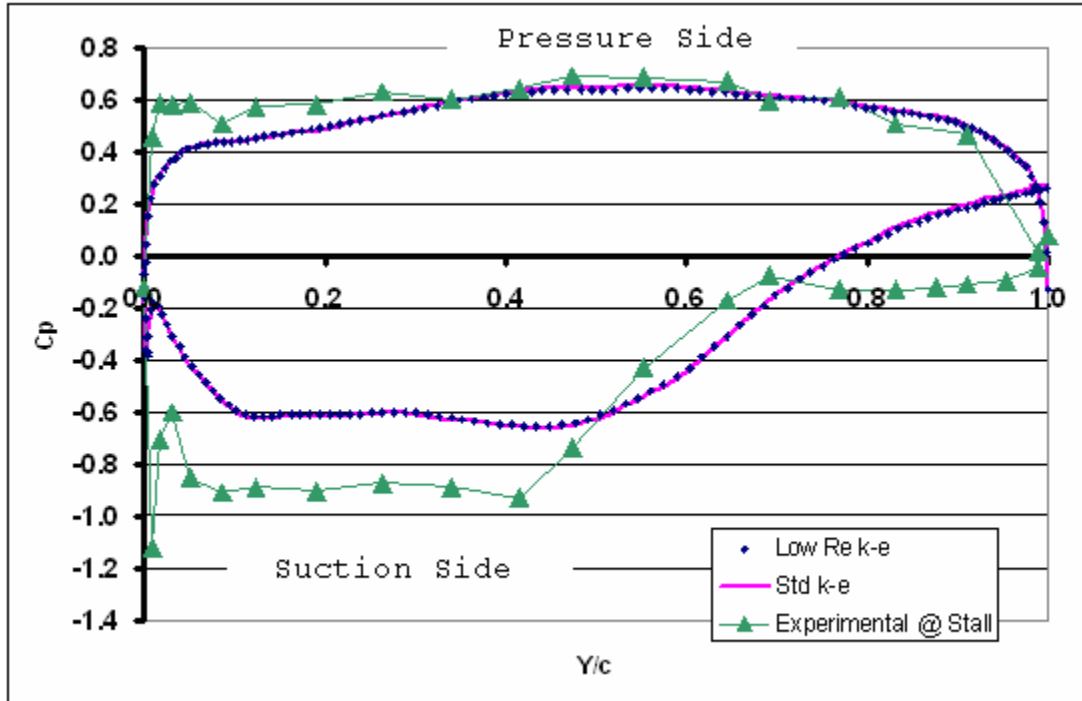
Figure 28.   CFD and Experimental Cp Distribution Comparison
at Stalled β_1

VI. CONCLUSIONS AND RECOMMENDATIONS

A.   CONCLUSIONS

The main objective of the study was achieved, in that continuous surveys in the inlet, boundary layer, and wake were successfully performed at $Re_c \approx 667,000$. Equipment troubleshooting showed that "Find" software required periodic re-installation in order for continuous surveys to be collected and processed with the personal computer used to process the data. The data collected showed good agreement with that obtained by Fitzgerald.

The secondary objectives of the study were successfully met. Inlet and wake data were obtained via continuous surveys at low and intermediate Re_c values, which gave a better understanding of the stalled flow of the test blades.

The third objective was partially met. Initial CFD predictions were made, but did not show close agreement with experimental data. However, the fact that the shapes of the Cp distributions were similar in shape, if different in magnitude, was an important first step towards the final solution. Groundwork has been laid for future research.

B.   RECOMMENDATIONS

Based on the interesting results of the flow seen at $Re_c \approx 545,000$, additional surveys should be conducted between Stations 11 and 12 over a range of intermediate Re_c. Two-component testing should be the first step, but a return to 3-component LDV measurements should be undertaken as soon as possible.

Further boundary layer testing should be performed at the full range of Re_c to supplement the inlet and wake data collected.

CFD efforts should be aggressively pursued to attempt to obtain better correlation between CFD predictions and experimental data. Several methods should be investigated, such as refined mesh grids, 3-D models, and testing with the remaining turbulence models that were not investigated during this study.

APPENDIX A. PROCESSOR CONTROL FREQUENCY AND COLORLINK FREQUENCY SHIFT SETTINGS

Tunnel Setting	Station #	Grid	Laser Orientation	Processor Control Freq (MHz)	Colorlink Freq Shift (MHz)
12"	1	NA	HORZ	3-20	1
12"	1	NA	VERT	3-20	1
12"	11	CSE	HORZ	3-20	5
12"	11	CSE	VERT	10-50	10
12"	11	FINE	HORZ	3-20	5
12"	11	FINE	VERT	3-20	5
12"	12	CSE	HORZ	1-10	5
12"	12	CSE	VERT	3-20	5
12"	12	FINE	HORZ	3-20	5
12"	12	FINE	VERT	3-20	5
12"	13	CSE	HORZ	3-20	10
12"	13	CSE	VERT	10-50	10
12"	13	FINE	HORZ	3-20	5
12"	13	FINE	VERT	3-20	5
12"	9	NA	VERT	3-20	5
12"	8	NA	VERT	5-30	2
12"	7	NA	VERT	5-30	2
2"	1	NA	HORZ	5-30	5
2"	1	NA	VERT	3-20	5
2"	11	FINE	HORZ	1-10	5
2"	11	FINE	VERT	3-20	5
2"	12	FINE	HORZ	1-10	5
2"	12	FINE	VERT	3-20	5
2"	13	FINE	HORZ	5-30	5
2"	13	FINE	VERT	3-20	2
8"	1	FINE	HORZ	5-30	10
8"	1	FINE	VERT	5-30	5
8"	11	FINE	HORZ	5-30	10
8"	11	FINE	VERT	3-20	5
8"	12	FINE	HORZ	5-30	10
8"	12	FINE	VERT	3-20	5
8"	13	NA	HORZ	5-30	10
8"	13	NA	VERT	5-30	5

THIS PAGE INTENTIONALLY LEFT BLANK
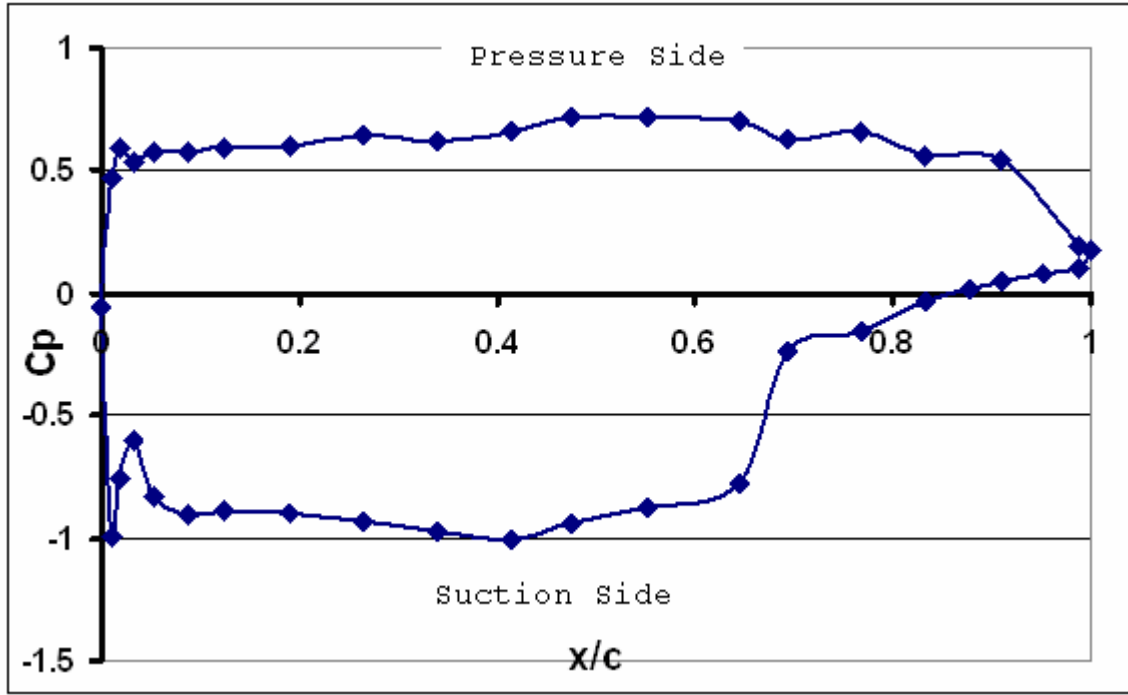
Figure 29.   Blade 6 Pressure Distribution @ $Re_c \approx 268,103$
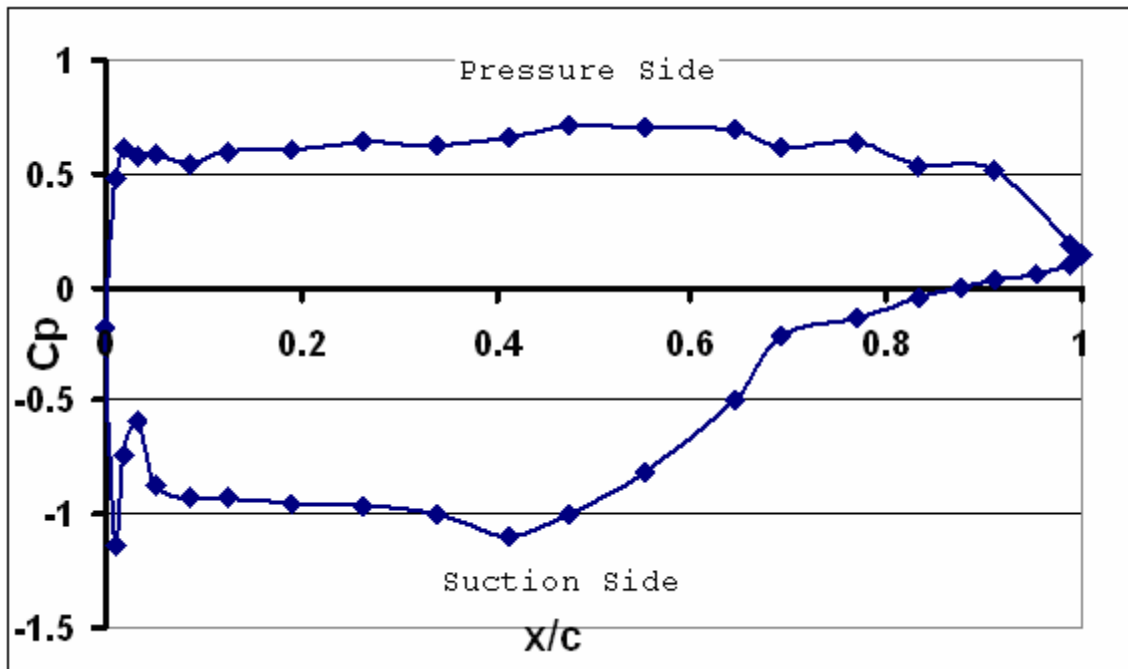
Figure 30.   Blade 6 Pressure Distribution @ $Re_c \approx 387,326$
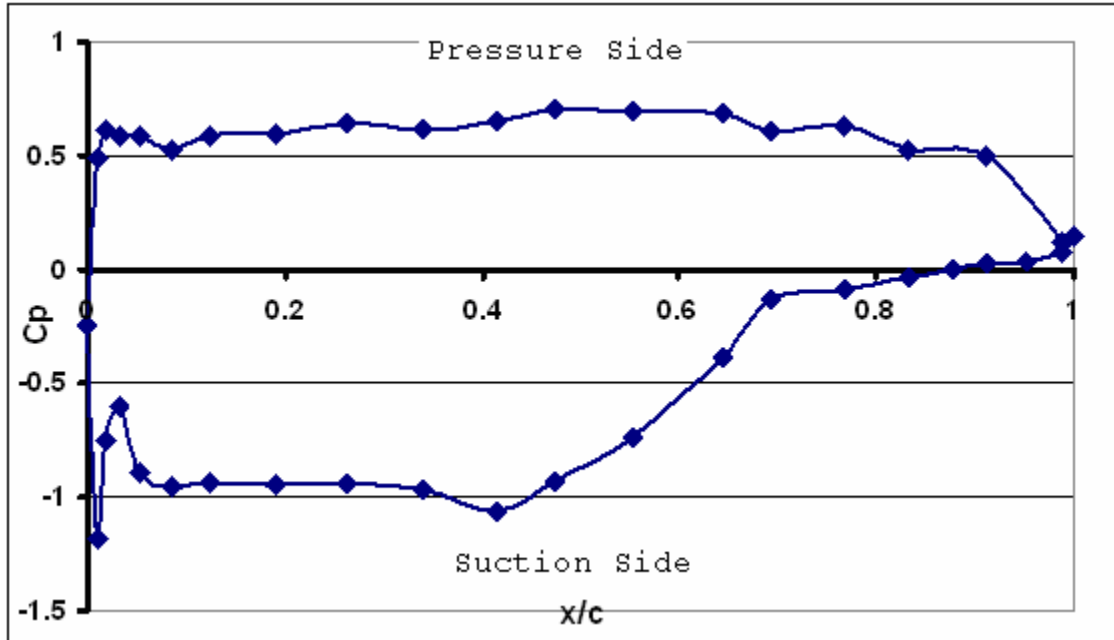
Figure 31.   Blade 6 Pressure Distribution @ $Re_c \approx 467,568$
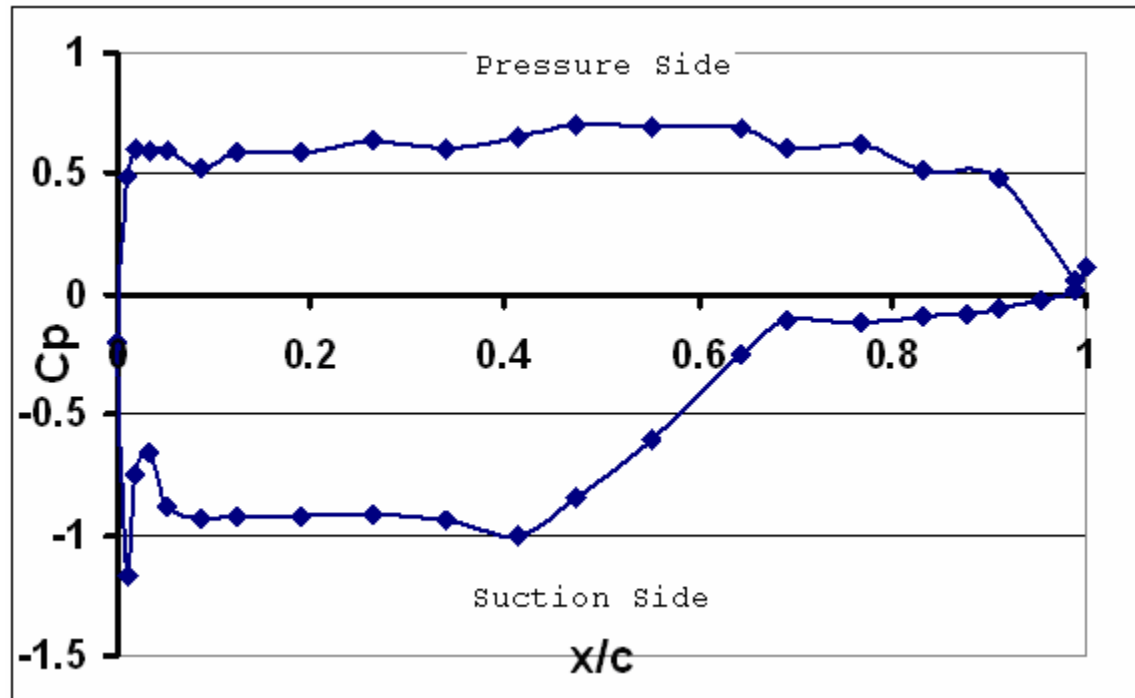
Figure 32.   Blade 6 Pressure Distribution @ $Re_c \approx 544,759$
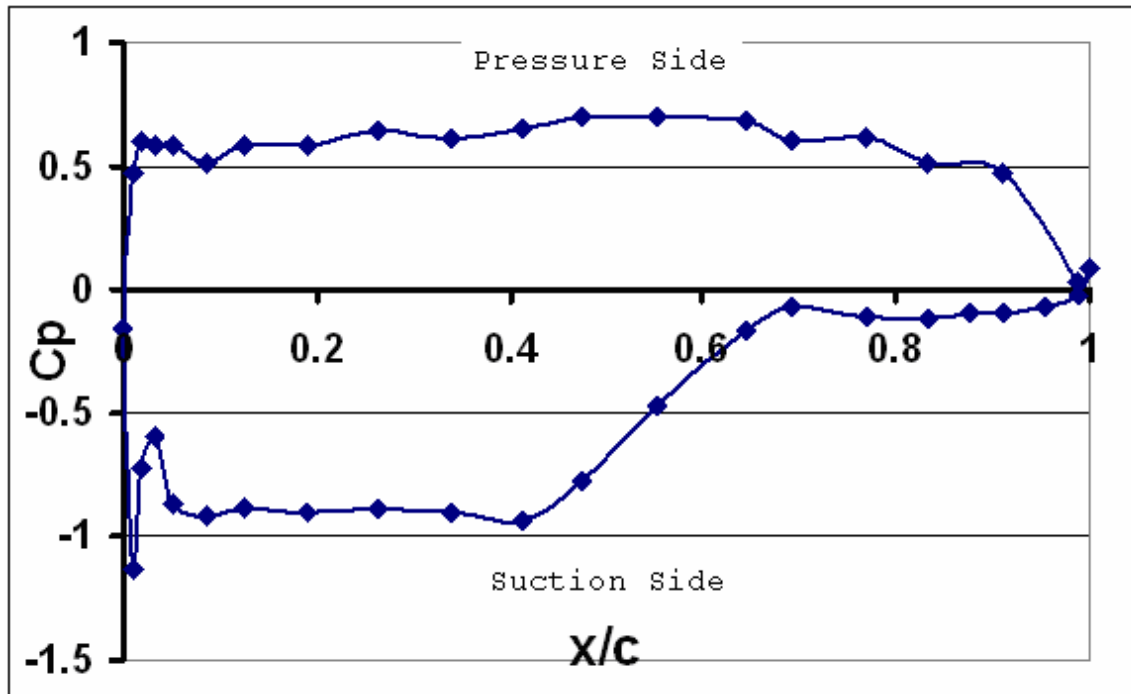
Figure 33.   Blade 6 Pressure Distribution @ $Re_c \approx 613,024$
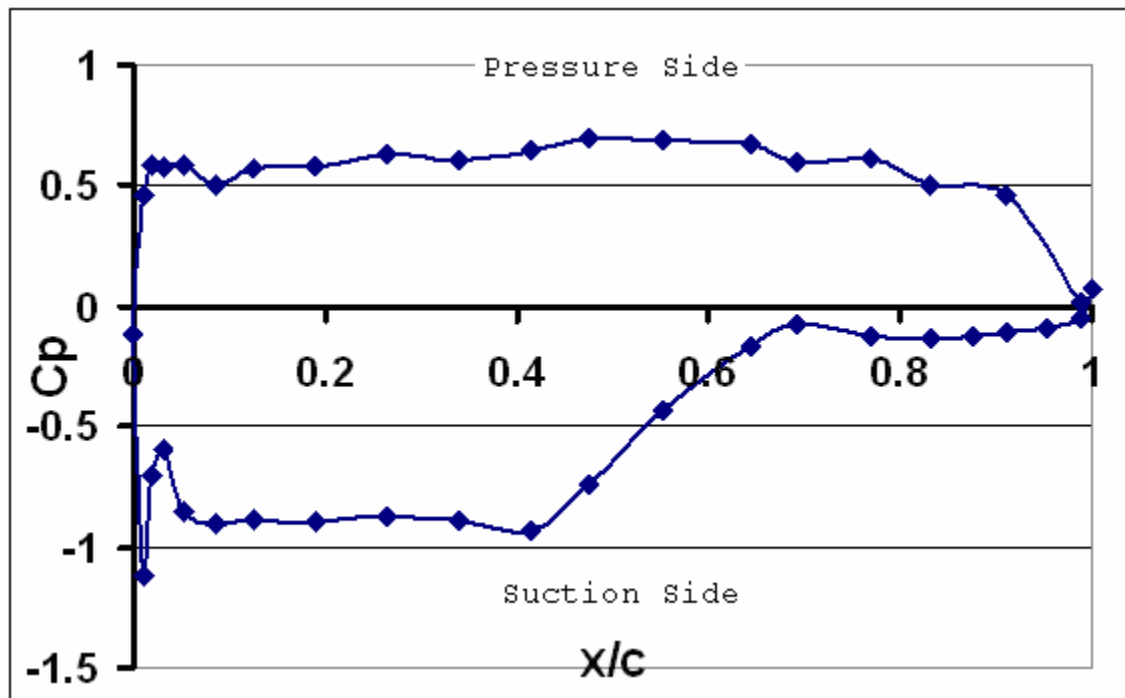
Figure 34.   Blade 6 Pressure Distribution @ $Re_c \approx 666,631$
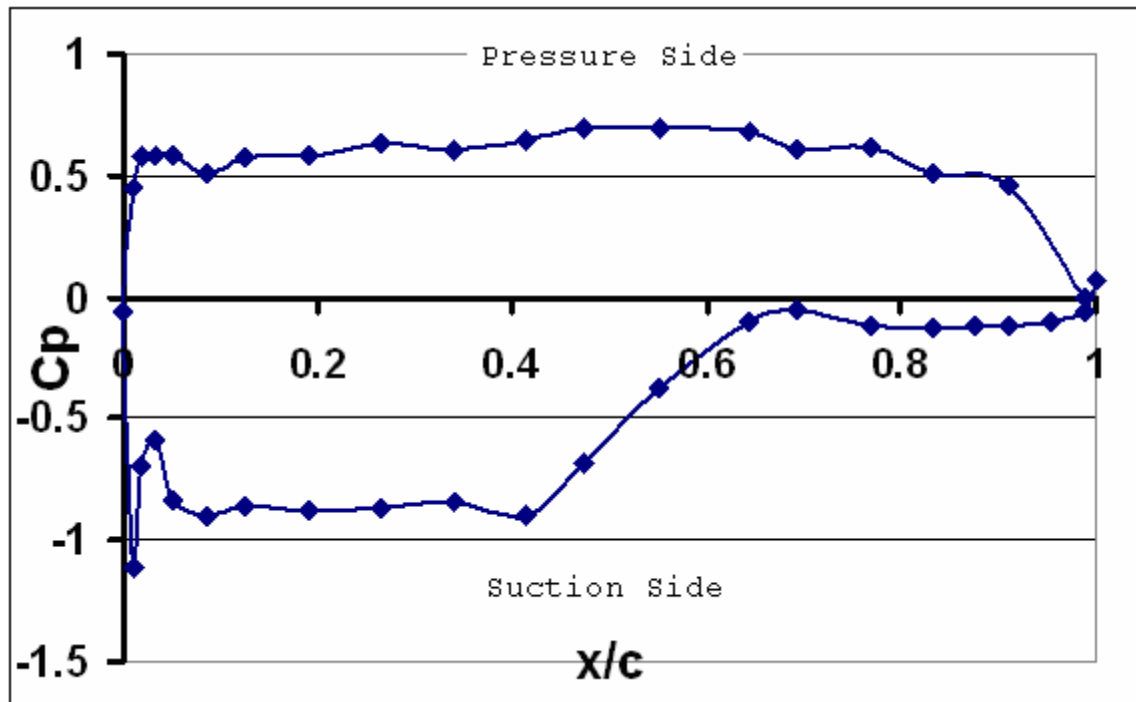
Figure 35.   Blade 6 Pressure Distribution @ $Re_c \approx 720{,}803$

APPENDIX C. LDV RAW DATA

A total of 33 LDV surveys were conducted, and the raw velocity data was collected using TSI Incorporated "Find" Version 1.6 software. The data was non-dimensionalized using the FORTRAN program "Calib1.for" and was recorded below. The details of "Calib.for" were contained in Hansen [Ref 1].

Reference Velocity	Tunnel Setting (" H_2O)	Station	Laser Orientation	Survey Type	Date (2006)
69.9155	12	1	Horizontal	N/A	10-Feb
70.6931	12	1	Vertical	N/A	10-Feb
72.6044	12	11	Horizontal	Coarse	1-Mar
71.7298	12	11	Vertical	Coarse	6-Mar
71.0137	12	11	Horizontal	Fine	15-Feb
70.8479	12	11	Vertical	Fine	15-Feb
71.3758	12	12	Horizontal	Coarse	7-Mar
70.4253	12	12	Vertical	Coarse	6-Mar
70.3211	12	12	Horizontal	Fine	16-Feb
70.2472	12	12	Vertical	Fine	16-Feb
70.0618	12	13	Horizontal	Coarse	17-Feb
70.1014	12	13	Vertical	Coarse	17-Feb
70.3803	12	13	Horizontal	Fine	17-Feb
70.3144	12	13	Vertical	Fine	16-Feb
69.9677	12	9	Vertical	N/A	10-Mar
71.117	12	8	Vertical	N/A	10-Mar
71.2307	12	7	Vertical	N/A	11-Mar
32.4166	2	1	Horizontal	Fine	22-Feb
30.5648	2	1	Vertical	Fine	22-Feb
31.6803	2	11	Horizontal	Fine	7-Mar
32.1434	2	11	Vertical	Fine	7-Mar
32.1029	2	12	Horizontal	Fine	7-Mar
32.1434	2	12	Vertical	Fine	7-Mar
32.1817	2	13	Horizontal	Fine	22-Feb
30.6977	2	13	Vertical	Fine	22-Feb
57.934	8	1	Horizontal	Fine	21-Feb
58.2156	8	1	Vertical	Fine	21-Feb
57.934	8	11	Horizontal	Fine	21-Feb
58.7807	8	11	Vertical	Fine	7-Mar
57.9451	8	12	Horizontal	Fine	21-Feb
58.4929	8	12	Vertical	Fine	7-Mar
57.6576	8	13	Horizontal	Fine	21-Feb
57.5636	8	13	Vertical	Fine	21-Feb

49

Station 1 @ 2" H$_2$O Plenum Pressure

U ref =   30.5648

V ref =   32.4166

y (mm)	x (mm)	y/s	U ref	V ref	Tu	Tv
0	-36.576	0.0000	0.698185	0.68832	1.568243	1.900603
6.349	-36.576	0.0417	0.702504	0.690985	1.425641	1.858371
12.699	-36.576	0.0833	0.710801	0.698926	1.581597	1.705246
19.05	-36.576	0.1250	0.720293	0.697269	1.424977	1.811122
25.399	-36.576	0.1667	0.731521	0.682842	1.687861	2.196489
31.75	-36.576	0.2083	0.728586	0.668296	1.598052	1.90802
38.1	-36.576	0.2500	0.727281	0.659606	1.755082	1.75299
44.45	-36.576	0.2917	0.733589	0.65224	1.573218	1.836982
50.799	-36.576	0.3333	0.731223	0.647643	1.759865	1.748702
57.149	-36.576	0.3750	0.733052	0.643152	1.906222	1.741315
63.5	-36.576	0.4167	0.733393	0.634909	1.977183	1.579254
69.849	-36.576	0.4583	0.734816	0.636671	1.817912	1.939821
76.2	-36.576	0.5000	0.727647	0.624665	1.667673	1.875087
82.549	-36.576	0.5417	0.726201	0.612091	1.495321	1.749973
88.9	-36.576	0.5833	0.711933	0.604678	1.394378	1.628095
95.25	-36.576	0.6250	0.708534	0.602077	1.59163	1.689838
101.599	-36.576	0.6667	0.700538	0.615265	1.668457	1.703287
107.95	-36.576	0.7083	0.699124	0.613244	1.723391	1.772546
114.299	-36.576	0.7500	0.692156	0.622814	1.851565	1.770329
120.65	-36.576	0.7917	0.691312	0.628604	2.03155	1.864213
127	-36.576	0.8333	0.685805	0.637908	1.79801	1.770826
133.349	-36.576	0.8750	0.674138	0.64529	1.725288	1.609049
139.699	-36.576	0.9167	0.672918	0.658231	1.478569	1.575916
146.05	-36.576	0.9583	0.673896	0.67884	1.628106	1.549304
152.4	-36.576	1.0000	0.682851	0.684208	1.549744	1.638521

Station 1 @ 8" H$_2$O

U ref = 58.2156

V ref = 57.934

y (mm)	x (mm)	y/s	U ref	V ref	Tu	Tv
0	-36.576	0.0000	0.721418	0.69041	1.694359	2.014022
6.349	-36.576	0.0417	0.727216	0.710907	1.537807	2.010986
12.699	-36.576	0.0833	0.732761	0.711011	1.431631	2.21054
19.05	-36.576	0.1250	0.733364	0.705472	1.511594	2.626768
25.399	-36.576	0.1667	0.734018	0.69947	1.586852	2.649991
31.75	-36.576	0.2083	0.739319	0.6804	1.701491	2.725649
38.1	-36.576	0.2500	0.752041	0.668873	1.845184	2.326007
44.45	-36.576	0.2917	0.761607	0.662557	1.633015	2.249714
50.799	-36.576	0.3333	0.772233	0.661418	1.590074	2.390048
57.149	-36.576	0.3750	0.771573	0.648274	1.547745	2.220909
63.5	-36.576	0.4167	0.770998	0.643001	1.48572	2.22268
69.849	-36.576	0.4583	0.761052	0.63092	1.397596	2.303015
76.2	-36.576	0.5000	0.752288	0.61539	1.397864	2.020011
82.549	-36.576	0.5417	0.756139	0.616869	1.591197	1.911147
88.9	-36.576	0.5833	0.743402	0.614542	1.438662	1.889263
95.25	-36.576	0.6250	0.737141	0.614824	1.611913	2.041836
101.599	-36.576	0.6667	0.73576	0.618863	1.91934	2.240036
107.95	-36.576	0.7083	0.733022	0.625721	1.811759	2.221158
114.299	-36.576	0.7500	0.721813	0.624409	1.564956	2.176702
120.65	-36.576	0.7917	0.717438	0.628405	1.750564	2.250179
127	-36.576	0.8333	0.71031	0.640206	1.572306	2.161137
133.349	-36.576	0.8750	0.704493	0.64932	1.599355	2.070129
139.699	-36.576	0.9167	0.704851	0.663874	1.595479	2.101202
146.05	-36.576	0.9583	0.708917	0.676435	1.561155	2.078976
152.4	-36.576	1.0000	0.723519	0.692459	1.559386	2.052475

Station 1 @ 12 " H_2O

U ref =	70.6931					
V ref =	69.9155					

y (mm)	x (mm)	y/s	U ref	V ref	Tu	Tv
0	-36.576	0.0000	0.74004	0.684117	1.525044	1.838948
6.349	-36.576	0.0417	0.740266	0.685334	1.478326	1.993789
12.699	-36.576	0.0833	0.741971	0.682211	1.511186	2.140845
19.05	-36.576	0.1250	0.742422	0.679208	1.540971	2.07217
25.399	-36.576	0.1667	0.747002	0.674301	1.627912	1.666589
31.75	-36.576	0.2083	0.754018	0.672665	1.84506	1.471993
38.1	-36.576	0.2500	0.764517	0.671092	1.664217	1.587084
44.45	-36.576	0.2917	0.772814	0.671266	1.76217	1.672211
50.799	-36.576	0.3333	0.778174	0.660227	1.620881	1.656609
57.149	-36.576	0.3750	0.774957	0.650471	1.529408	1.670552
63.5	-36.576	0.4167	0.774698	0.644472	1.330404	1.604858
69.849	-36.576	0.4583	0.769296	0.635747	1.337836	1.55596
76.2	-36.576	0.5000	0.770105	0.633247	1.495667	1.641421
82.549	-36.576	0.5417	0.769607	0.63464	1.847795	1.560149
88.9	-36.576	0.5833	0.768054	0.634311	1.894512	1.706697
95.25	-36.576	0.6250	0.769282	0.636803	1.952067	1.801579
101.599	-36.576	0.6667	0.765772	0.638328	1.992516	1.815589
107.95	-36.576	0.7083	0.756587	0.636397	1.724111	1.880247
114.299	-36.576	0.7500	0.747346	0.641328	1.538255	1.757221
120.65	-36.576	0.7917	0.740142	0.646376	1.440804	1.563745
127	-36.576	0.8333	0.733154	0.652413	1.650153	1.516639
133.349	-36.576	0.8750	0.728716	0.662395	1.537183	1.452481
139.699	-36.576	0.9167	0.729572	0.673802	1.639188	1.267745
146.05	-36.576	0.9583	0.728702	0.681425	1.586034	1.585861
152.4	-36.576	1.0000	0.731609	0.688165	1.64909	1.703848

Station 7 @ 12" H$_2$O
U ref = 71.2307

y (mm)	x (mm)	y/s	d/c	U mean	U TI%	U ref	Tu
67.149	56.908	0.4406	0.212749	67.8427	4.28027	0.952436	4.076684
66.159	57.058	0.4341	0.204873	67.6946	5.17435	0.950357	4.91748
65.168	57.209	0.4276	0.196998	68.5369	3.51181	0.962182	3.379
64.179	57.359	0.4211	0.189122	68.8312	4.05997	0.966314	3.923205
63.189	57.509	0.4146	0.181247	69.0427	4.24099	0.969283	4.110719
62.198	57.658	0.4081	0.173371	69.2018	4.15843	0.971516	4.039983
61.209	57.808	0.4016	0.165496	69.3937	4.07023	0.974211	3.965261
60.219	57.959	0.3951	0.157621	69.9191	3.83072	0.981587	3.760183
59.228	58.109	0.3886	0.149745	69.8683	5.14729	0.980873	5.04884
58.238	58.259	0.3821	0.141870	70.1593	3.97812	0.984959	3.918284
57.249	58.408	0.3756	0.133994	70.3426	3.5994	0.987532	3.554523
56.259	58.558	0.3692	0.126119	70.6734	3.50504	0.992176	3.477617
55.268	58.709	0.3627	0.118244	70.9525	4.22289	0.996094	4.206397
54.279	58.859	0.3562	0.110368	71.1627	4.35306	0.999045	4.348904
53.289	59.009	0.3497	0.102493	72.3361	3.8651	1.015519	3.925081
52.298	59.158	0.3432	0.094618	71.1461	6.64314	0.998812	6.63525
51.308	59.308	0.3367	0.086743	71.6104	4.27474	1.005331	4.297527
50.319	59.459	0.3302	0.078868	70.5821	7.98666	0.990894	7.913936
49.329	59.609	0.3237	0.070993	72.4072	6.27903	1.016517	6.382739
48.338	59.759	0.3172	0.063118	69.8954	9.22642	0.981254	9.05346
47.348	59.908	0.3107		72.0255	4.38215	1.011158	4.431047
46.359	60.058	0.3042	0.055243	71.483	6.38379	1.003542	6.406401
45.368	60.209	0.2977	0.047369	72.4157	4.51958	1.016636	4.594768
44.378	60.359	0.2912	0.039495	71.5586	6.71085	1.004603	6.741742
43.389	60.509	0.2847	0.023751	62.1129	11.3923	0.871996	9.934042
42.399	60.658	0.278209	0.015884	46.4472	16.8434	0.652067	10.98303
41.408	60.808	0.271706	0.008035	43.2364	19.7344	0.606991	11.9786
40.418	60.959	0.26521	0.000925	31.0678	20.9916	0.436157	9.155643

Station 8 @ 12" H₂O

U ref =   71.2307

y (mm)	x (mm)	y/s	d/c	U mean	U TI%	U ref	Tu
75.686	93.748	0.4966	0.275406	64.3528	1.37613	0.904886	1.245241
74.688	93.683	0.4901	0.267540	64.4283	1.35717	0.905948	1.229525
73.689	93.617	0.4835	0.259681	64.5423	1.29101	0.907551	1.171657
72.691	93.551	0.4770	0.251807	64.5798	1.37136	0.908078	1.245302
71.694	93.483	0.4704	0.243940	64.5703	1.30774	0.907945	1.187356
70.695	93.418	0.4639	0.236081	64.623	2.8979	0.908686	2.63328
69.697	93.352	0.4573	0.228206	64.6712	2.60525	0.909363	2.369119
68.7	93.287	0.4508	0.220340	64.6988	1.37349	0.909752	1.249535
67.701	93.221	0.4442	0.212481	64.6103	1.87928	0.908507	1.707339
66.703	93.155	0.4377	0.204607	64.6857	1.54104	0.909567	1.40168
65.706	93.087	0.4311	0.196740	64.6286	2.4114	0.908764	2.191395
64.707	93.022	0.4246	0.188881	64.5166	3.49744	0.90719	3.172841
63.71	92.956	0.4180	0.181007	64.1992	3.41896	0.902726	3.086386
62.712	92.891	0.4115	0.173149	63.9511	4.94197	0.899238	4.444007
61.713	92.825	0.4049	0.165282	63.83	4.13514	0.897535	3.711433
60.716	92.759	0.3984	0.157408	62.9572	5.93429	0.885262	5.253403
59.718	92.691	0.3919	0.149549	62.4595	7.13281	0.878264	6.26449
58.719	92.626	0.3853	0.141674	61.267	9.96809	0.861496	8.587468
57.722	92.561	0.3788	0.133809	58.5196	14.9419	0.822864	12.29515
56.723	92.495	0.3722	0.125950	54.3084	20.3884	0.763649	15.56957
55.725	92.429	0.3656	0.118076	50.0596	24.3938	0.703905	17.17091
54.728	92.361	0.3591	0.110209	45.4988	26.9358	0.639774	17.23282
53.729	92.296	0.3526	0.102351	41.4049	29.2389	0.582208	17.02313
52.731	92.23	0.3460	0.094477	36.259	32.7287	0.50985	16.68673
51.734	92.165	0.3395	0.086612	33.7014	34.4537	0.473887	16.32715
50.735	92.099	0.332907	0.078754	28.576	40.9291	0.401817	16.446
49.737	92.033	0.326358	0.070881	23.0649	59.2936	0.324323	19.2303
48.74	91.965	0.319816	0.063015	15.667	93.1609	0.220299	20.52325
47.741	91.9	0.313261	0.055158	3.23092	379.75	0.045431	17.25244
46.743	91.834	0.306713	0.047286	-2.77343	264.804	-0.039	10.32686
45.746	91.769	0.300171	0.039424	-5.00737	72.7185	-0.07041	5.120132
44.747	91.703	0.293615	0.031571	-5.45367	55.6714	-0.07669	4.269211
43.75	91.637	0.287073	0.023707	-5.90554	34.1861	-0.08304	2.838806
42.753	91.569	0.280531	0.015867	-5.67365	44.1336	-0.07978	3.520939

54

Station 9 @ 12" H₂O
U ref =   71.2307

y (mm)	x (mm)	y/s	d/c	U mean	U TI%	U ref	Tu
80.001	119.021	0.5249	0.322907	63.8225	1.97118	0.912171	1.798053
79.003	118.942	0.5184	0.315034	63.9329	2.48166	0.913749	2.267614
78.004	118.864	0.5118	0.307160	63.8437	2.13732	0.912474	1.950249
77.007	118.787	0.5053	0.299287	63.7196	2.96848	0.9107	2.703395
76.009	118.709	0.4987	0.291413	63.5604	3.07285	0.908425	2.791453
75.01	118.631	0.4922	0.283540	63.3182	4.07536	0.904963	3.688051
74.013	118.552	0.4856	0.275666	63.2586	4.15426	0.904111	3.755914
73.015	118.474	0.4791	0.267793	62.607	5.82102	0.894799	5.208641
72.016	118.397	0.4725	0.259919	62.5804	6.22097	0.894418	5.56415
71.019	118.319	0.4660	0.252046	61.2919	8.71406	0.876003	7.633541
70.021	118.24	0.4595	0.244172	59.6075	11.5608	0.851929	9.848979
69.022	118.162	0.4529	0.236299	57.3668	15.4615	0.819904	12.67695
68.025	118.084	0.4464	0.228425	55.7028	18.2955	0.796122	14.56544
67.027	118.007	0.4398	0.220552	51.746	22.7482	0.73957	16.82388
66.028	117.929	0.4333	0.212678	50.0706	24.0244	0.715624	17.19245
65.031	117.85	0.4267	0.204805	48.5258	26.0112	0.693546	18.03996
64.033	117.772	0.4202	0.196931	46.6226	26.6318	0.666345	17.74596
63.034	117.694	0.4136	0.189058	44.42	28.1315	0.634864	17.85969
62.036	117.617	0.4071	0.181184	41.3973	31.7672	0.591663	18.79548
61.039	117.539	0.4005	0.173311	38.977	32.2542	0.557071	17.96789
60.04	117.46	0.3940	0.165438	38.5592	32.043	0.5511	17.6589
59.042	117.382	0.3874	0.157564	36.0093	34.0975	0.514656	17.54848
58.045	117.305	0.3809	0.149691	32.7987	35.4545	0.468769	16.61998
57.046	117.227	0.3743	0.141817	33.1675	37.5199	0.47404	17.78594
56.048	117.149	0.3678	0.133936	29.3453	40.2485	0.419412	16.88071
55.051	117.069	0.361227	0.126070	25.9667	45.9906	0.371124	17.06822
54.052	116.992	0.354672	0.118189	24.5059	51.2979	0.350246	17.96688
53.054	116.915	0.348123	0.110316	17.2197	77.6507	0.246109	19.11056
52.057	116.837	0.341581	0.102451	13.0643	111.607	0.186719	20.83915
51.058	116.759	0.335026	0.094570	6.34142	205.769	0.090634	18.64957
50.06	116.68	0.328478	0.086696	2.18765	521.288	0.031267	16.29889
49.063	116.602	0.321936	0.078831	-0.95783	891.17	-0.01369	12.1998
48.064	116.525	0.315381	0.070951	-2.78616	220.732	-0.03982	8.789694
47.067	116.447	0.308839	0.063086	-3.8665	129.129	-0.05526	7.135825
46.069	116.367	0.30229	0.055213	-4.58406	87.7352	-0.06552	5.74813
45.07	116.29	0.295735	0.047333	-4.77854	79.5809	-0.0683	5.435087
44.073	116.212	0.289193	0.039469	-5.27592	62.0777	-0.07541	4.680974
43.075	116.135	0.282644	0.031599	-5.20845	55.232	-0.07444	4.111513
42.076	116.057	0.276089	0.023722	-5.58194	46.7522	-0.07978	3.729835
41.079	115.977	0.269547	0.015865	-5.70848	46.7372	-0.08159	3.813165
40.081	115.9	0.262999	0.008019	-5.7838	44.4405	-0.08266	3.673623
39.082	115.822	0.256444	0.000949	28.2914	22.4424	0.404349	9.074572

Station 11 @ 2" H$_2$O

U ref = 30.5823
V ref = 31.9608

y (mm)	x (mm)	y/s	U ref	V ref	Tu	Tv
0	134.111	0	0.855819	0.114572	2.281612	1.997407
2.5	134.111	0.016404	0.85851	0.108944	2.631804	2.131138
5	134.111	0.032808	0.856057	0.109776	2.200975	2.456371
7.5	134.111	0.049213	0.861587	0.101302	2.156741	2.241791
10	134.111	0.065617	0.857787	0.096305	2.251537	2.270522
12.5	134.111	0.082021	0.856947	0.098309	2.27767	2.709649
15	134.111	0.098425	0.866583	0.081661	2.30297	2.188579
17.5	134.111	0.114829	0.882095	0.085797	2.267302	2.230404
20	134.111	0.131234	0.89062	0.069091	2.446256	2.312963
22.5	134.111	0.147638	0.889413	0.073817	2.368054	2.12159
25	134.111	0.164042	0.90437	0.06014	2.642577	2.222555
27.5	134.111	0.180446	0.901083	0.052711	2.876438	2.403589
30	134.111	0.19685	0.943418	0.047555	3.054534	2.382468
32.5	134.111	0.213255	0.955661	0.052581	4.192158	2.544299
35	134.111	0.229659	0.837056	0.027873	14.25297	6.274083
37.5	134.111	0.246063	0.985642	-0.05516	19.03403	-10.8149
37.5	134.111	0.246063	-0.10456	-0.04107	-16.2391	-9.50018
40	134.111	0.262467	0.082068	-0.01756	33.97401	-9.88609
42.5	134.111	0.278871	0	-0.00077	0	-7.80085
45	134.111	0.295276	0.265363	0.008692	42.29196	9.579562
47.5	134.111	0.31168	0.463395	0.010359	43.95065	4.240527
50	134.111	0.328084	0.890924	0.016524	13.71444	2.120991
52.5	134.111	0.344488	0.823738	0.030415	22.53055	3.390218
55	134.111	0.360892	0.826481	0.037138	22.39161	3.286001
57.5	134.111	0.377297	0.876906	0.04161	16.60378	1.719756
60	134.111	0.393701	0.884633	0.049888	13.968	1.992638
62.5	134.111	0.410105	0.939468	0.073936	8.945607	2.123292
65	134.111	0.426509	0.93815	0.072632	9.264968	2.172847
67.5	134.111	0.442913	0.939782	0.072983	7.030557	1.759748
70	134.111	0.459318	0.941983	0.089343	5.346374	2.219599
72.5	134.111	0.475722	0.943471	0.095709	4.140996	2.540626
75	134.111	0.492126	0.930457	0.090536	3.466313	2.033907
77.5	134.111	0.50853	0.932794	0.08977	3.258643	1.734924
80	134.111	0.524934	0.916226	0.098264	2.524331	2.435113
82.5	134.111	0.541339	0.912472	0.108328	2.481477	2.787407
85	134.111	0.557743	0.898513	0.105278	2.474083	2.689556
87.5	134.111	0.574147	0.909144	0.115719	2.605669	2.332848
90	134.111	0.590551	0.90694	0.105625	2.670692	2.350854
92.5	134.111	0.606955	0.897555	0.111015	2.375694	2.680155
95	134.111	0.62336	0.885094	0.111422	2.236446	2.232536
97.5	134.111	0.639764	0.880513	0.117238	2.396077	2.387369

Station 11 @ 8" H$_2$O

U ref =   58.7808

V ref =   57.934

y (mm)	x (mm)	y/s	U/Uref	V/Vref	Tu	Tv
0	128.014	0	0.862234	0.160156	2.450865	1.998903
2.5	128.014	0.016404	0.864092	0.15162	3.259172	2.017314
5	128.014	0.032808	0.869148	0.147969	2.814387	2.199558
7.5	128.014	0.049213	0.859883	0.139881	3.490411	2.123218
10	128.014	0.065617	0.869177	0.133259	3.277152	2.318873
12.5	128.014	0.082021	0.86352	0.1264	3.781043	2.139767
15	128.014	0.098425	0.870903	0.118575	2.762732	2.179487
17.5	128.014	0.114829	0.874136	0.112485	2.608815	2.370398
20	128.014	0.131234	0.878411	0.105288	3.063098	2.247603
22.5	128.014	0.147638	0.891579	0.098912	3.876138	2.283992
25	128.014	0.164042	0.904906	0.089309	3.507217	2.474517
27.5	128.014	0.180446	0.912036	0.083642	3.74046	2.486088
30	128.014	0.19685	0.932621	0.079162	5.619973	2.450578
32.5	128.014	0.213255	0.953439	0.07706	5.199236	2.639185
35	128.014	0.229659	0.805164	0.107981	16.00852	5.398725
37.5	128.014	0.246063	0.736528	0.046385	15.25386	14.78878
37.5	128.014	0.246063	0.214335	-0.00937	35.06718	11.21087
40	128.014	0.262467	0.107377	0.013045	26.72306	11.47837
42.5	128.014	0.278871	-0.11847	0.03928	7.519419	11.07061
45	128.014	0.295276	-0.10064	0.073119	9.10046	11.864
47.5	128.014	0.31168	0.109229	0.096537	17.76507	12.66564
50	128.014	0.328084	0.257293	0.133963	22.40092	13.77981
52.5	128.014	0.344488	0.375327	0.180694	21.05838	15.67609
55	128.014	0.360892	0.470087	0.198661	18.59355	15.07943
57.5	128.014	0.377297	0.566263	0.187672	18.33384	14.62426
60	128.014	0.393701	0.650593	0.214615	18.16307	14.04631
62.5	128.014	0.410105	0.740842	0.195474	17.70628	13.28777
65	128.014	0.426509	0.838782	0.179326	14.75116	8.400029
67.5	128.014	0.442913	0.890228	0.161572	10.739	5.710731
70	128.014	0.459318	0.916053	0.175241	8.666049	4.305018
72.5	128.014	0.475722	0.910768	0.178172	6.659621	4.156408
75	128.014	0.492126	0.918861	0.186509	5.141314	3.59533
77.5	128.014	0.50853	0.911927	0.158568	4.547087	2.557977
80	128.014	0.524934	0.90566	0.162304	3.364607	2.935047
82.5	128.014	0.541339	0.894665	0.184546	3.790175	2.415341
85	128.014	0.557743	0.889852	0.179005	4.079623	2.412331
87.5	128.014	0.574147	0.88254	0.179558	3.074513	2.39302
90	128.014	0.590551	0.877491	0.174723	3.734302	1.996035
92.5	128.014	0.606955	0.863517	0.181465	3.497648	2.119313
95	128.014	0.62336	0.859883	0.177114	3.280539	2.082307
97.5	128.014	0.639764	0.856354	0.177397	2.15195	2.44646

Station 11 - Coarse Grid @ 12" H$_2$O
U ref = 71.7298
V ref = 72.6044

y (mm)	x (mm)	y/s	U ref	V ref	Tu	Tv
0	134.111	0	0.862271	0.157555	1.703062	2.03065
5	134.111	0.032808	0.865795	0.147703	1.785823	2.026089
10	134.111	0.065617	0.864632	0.128456	2.358034	2.13706
15	134.111	0.098425	0.873111	0.109252	1.817678	2.130374
20	134.111	0.131234	0.881339	0.089862	1.709234	2.155029
25	134.111	0.164042	0.894953	0.065918	1.771219	1.862612
30	134.111	0.19685	0.427	0.048454	4.951018	1.675402
35	134.111	0.229659	0.232998	0.000991	3.308688	0.053847
40	134.111	0.262467	-0.0935	-0.04835	5.846249	4.363938
45	134.111	0.295276	-0.1145	-0.02555	4.826715	5.748688
50	134.111	0.328084	-0.06294	0.042072	7.509014	10.78596
55	134.111	0.360892	0.05149	0.14237	11.9035	14.91769
60	134.111	0.393701	0.148403	0.28686	9.713079	9.810699
65	134.111	0.426509	0.212054	0.332221	6.184749	7.533209
70	134.111	0.459318	0.193489	0.310724	7.587579	7.669808
75	134.111	0.492126	0.876282	0.259493	3.66737	6.923806
80	134.111	0.524934	0.893064	0.217853	2.011457	4.002137
85	134.111	0.557743	0.890354	0.207343	1.781936	2.635783
90	134.111	0.590551	0.880302	0.20029	2.019096	2.286044
95	134.111	0.62336	0.867199	0.193435	2.170339	2.684079
100	134.111	0.656168	0.848041	0.184523	2.315703	2.666232
105	134.111	0.688976	0.830087	0.17712	2.289215	2.704181
110	134.111	0.721785	0.816231	0.162727	2.008051	1.997523
115	134.111	0.754593	0.816213	0.15731	2.154917	1.842871
120	134.111	0.787402	0.815749	0.153832	2.092592	1.687463
125	134.111	0.82021	0.815537	0.149983	2.018813	1.666142
130	134.111	0.853018	0.817125	0.145455	2.228536	1.843196
135	134.111	0.885827	0.810963	0.138989	2.055434	1.85803
140	134.111	0.918635	0.806694	0.131106	2.092822	1.825199
145	134.111	0.951444	0.800628	0.123024	1.91479	1.861762
150	134.111	0.984252	0.800574	0.114173	1.985671	1.797765
155	134.111	1.01706	0.803297	0.105511	2.179327	1.888728
160	134.111	1.049869	0.822205	0.093101	1.874085	2.039743
165	134.111	1.082677	0.835742	0.0815	2.077454	2.053771
170	134.111	1.115486	0.856329	0.076349	2.201973	2.518418
175	134.111	1.148294	0.880584	0.063627	2.21488	2.386084
180	134.111	1.181102	0.887448	0.054954	4.098104	5.908966
185	134.111	1.213911	0.750996	0.048358	10.7846	0.825949
190	134.111	1.246719	0.698758	-0.03137	4.194046	2.772688
195	134.111	1.279528	0.698024	-0.00617	3.814727	0.46551
200	134.111	1.312336	-0.09074	0.037702	5.454211	0.624959
205	134.111	1.345144	-0.06225	0.133026	7.006157	2.420016
210	134.111	1.377953	0.055988	0.229307	13.06221	15.85596
215	134.111	1.410761	0.147255	0.313723	11.06636	9.80966
220	134.111	1.44357	0.2151	0.323734	6.667851	8.612129
225	134.111	1.476378	0.779786	0.294765	8.039906	7.611527
230	134.111	1.509186	0.855384	0.251339	4.981703	4.785264
235	134.111	1.541995	0.889043	0.22312	2.109664	2.983316
240	134.111	1.574803	0.887336	0.212869	1.723064	2.131198
245	134.111	1.607612	0.88426	0.206131	1.676186	2.002649

Station 11 - Fine Grid @ 12" H$_2$O

U ref = 70.8479

V ref = 71.0137

y (mm)	x (mm)	y/s	U ref	V ref	Tu	Tv
0	128.014	0	0.868953	0.161318	1.661447	1.855143
2.5	128.014	0.016404	0.869004	0.154136	1.699328	1.918567
5	128.014	0.032808	0.870839	0.150461	1.690655	1.993008
7.5	128.014	0.049213	0.8707	0.140213	1.859668	2.041278
10	128.014	0.065617	0.869886	0.13352	2.003661	2.110237
12.5	128.014	0.082021	0.871063	0.125194	2.211072	2.214086
15	128.014	0.098425	0.873365	0.115518	2.619799	2.141654
17.5	128.014	0.114829	0.876798	0.102263	2.307092	2.274263
20	128.014	0.131234	0.882488	0.092455	2.425076	2.231841
22.5	128.014	0.147638	0.885673	0.080185	2.838521	2.181792
25	128.014	0.164042	0.887297	0.06892	3.464254	2.217407
27.5	128.014	0.180446	0.884232	0.056062	4.030905	2.063907
30	128.014	0.19685	0.881116	0.050151	5.052917	1.924431
32.5	128.014	0.213255	0.84397	0.048889	12.39733	2.446411
35	128.014	0.229659	0.71733	0.090189	18.08718	7.760917
37.5	128.014	0.246063	0.430761	-0.0403	8.283358	5.45657
37.5	128.014	0.246063	0.05145	-0.04907	19.67949	4.701913
40	128.014	0.262467	0	-0.03752	0	5.225927
42.5	128.014	0.278871	-0.05215	-0.00708	6.669714	8.183636
45	128.014	0.295276	-0.03837	0.018335	8.606519	10.01076
47.5	128.014	0.31168	-0.01208	0.070986	11.25223	12.69008
50	128.014	0.328084	0.042966	0.141432	15.65125	15.12741
52.5	128.014	0.344488	0.138754	0.205097	18.65875	14.62014
55	128.014	0.360892	0.274616	0.281091	18.30453	10.97842
57.5	128.014	0.377297	0.355573	0.323887	16.18479	8.376166
60	128.014	0.393701	0.434686	0.333864	15.19298	8.543707
62.5	128.014	0.410105	0.492438	0.336758	15.89595	8.528789
65	128.014	0.426509	0.556952	0.313227	16.50044	10.13821
67.5	128.014	0.442913	0.651617	0.278134	17.07791	9.544295
70	128.014	0.459318	0.749475	0.243357	15.96298	6.833083
72.5	128.014	0.475722	0.825811	0.216472	12.08278	4.611272
75	128.014	0.492126	0.875065	0.211378	7.486905	3.687396
77.5	128.014	0.50853	0.888337	0.203483	5.680239	3.104443
80	128.014	0.524934	0.900212	0.199067	2.609308	2.90035
82.5	128.014	0.541339	0.901332	0.198143	1.925489	2.768976
85	128.014	0.557743	0.901674	0.195431	2.145371	2.543753
87.5	128.014	0.574147	0.898192	0.190367	1.734552	2.609291
90	128.014	0.590551	0.889419	0.189877	1.812984	2.703513
92.5	128.014	0.606955	0.885009	0.18379	2.236815	2.95071
95	128.014	0.62336	0.877069	0.179736	1.992964	2.979803
97.5	128.014	0.639764	0.869381	0.174858	2.217764	2.742487

Station 12 @ 2" H$_2$O

U ref = 31.2339

V ref = 31.9578

y (mm)	x (mm)	y/s	U ref	V ref	Tu	Tv
0	134.111	0	0.82182	0.126027	2.076855	1.937593
2.5	134.111	0.016404	0.829797	0.125027	2.032945	1.933193
5	134.111	0.032808	0.832193	0.118041	2.036217	1.929558
7.5	134.111	0.049213	0.842192	0.118649	2.210391	2.341985
10	134.111	0.065617	0.824297	0.105021	2.170612	2.236724
12.5	134.111	0.082021	0.831682	0.103167	2.172853	2.28855
15	134.111	0.098425	0.838051	0.103616	2.248658	2.68777
17.5	134.111	0.114829	0.839538	0.107298	2.260002	2.817404
20	134.111	0.131234	0.83914	0.084329	2.428101	2.427177
22.5	134.111	0.147638	0.856552	0.091227	2.593546	2.729912
25	134.111	0.164042	0.850367	0.088662	2.668181	3.017509
27.5	134.111	0.180446	0.845172	0.099068	2.690858	3.230489
30	134.111	0.19685	0.884362	0.098213	3.725339	3.715621
32.5	134.111	0.213255	0.878134	0.112467	5.908777	5.297084
35	134.111	0.229659	0.812073	0.112459	11.73154	12.67439
37.5	134.111	0.246063	0.262245	0.015998	29.32297	17.53172
37.5	134.111	0.246063	-0.05201	-0.04817	19.12232	12.91887
40	134.111	0.262467	0.113721	-0.05522	34.0558	13.6497
42.5	134.111	0.278871	0	-0.03312	0	12.01823
45	134.111	0.295276	0.486601	-0.0122	38.71191	11.34265
47.5	134.111	0.31168	0.613734	-0.01116	34.41164	15.33446
50	134.111	0.328084	0.774075	0.012561	22.59401	10.88983
52.5	134.111	0.344488	0.755079	0.028221	21.9447	6.471196
55	134.111	0.360892	0.767003	0.036322	17.91735	5.256286
57.5	134.111	0.377297	0.838514	0.048174	11.04424	6.073114
60	134.111	0.393701	0.873072	0.057029	6.09763	6.661192
62.5	134.111	0.410105	0.874319	0.053704	7.222272	2.085331
65	134.111	0.426509	0.873713	0.077936	5.652013	5.157323
67.5	134.111	0.442913	0.866766	0.06811	6.644722	1.845714
70	134.111	0.459318	0.881406	0.086925	5.235916	4.092327
72.5	134.111	0.475722	0.87109	0.096017	3.09994	3.638466
75	134.111	0.492126	0.862273	0.094746	2.962384	3.330205
77.5	134.111	0.50853	0.869737	0.087622	3.437244	1.839299
80	134.111	0.524934	0.854611	0.107506	2.968611	2.748688
82.5	134.111	0.541339	0.862208	0.099532	2.66712	2.249071
85	134.111	0.557743	0.848653	0.10361	2.235862	2.157197
87.5	134.111	0.574147	0.853572	0.102401	2.735322	2.641435
90	134.111	0.590551	0.840372	0.109427	2.216026	2.471654
92.5	134.111	0.606955	0.842167	0.106912	2.218688	2.050528
95	134.111	0.62336	0.838589	0.101899	2.285105	2.029806
97.5	134.111	0.639764	0.839242	0.104947	2.419468	2.324378

Station 12 @ 8" H_2O

U ref = 57.5718

V ref = 57.9451

y (mm)	x (mm)	y/s	U ref	V ref	Tu	Tv
0	134.111	0	0.863356	0.160799	2.910555	2.024509
2.5	134.111	0.016404	0.875352	0.15004	1.954356	1.984056
5	134.111	0.032808	0.877048	0.153412	1.861474	2.064326
7.5	134.111	0.049213	0.879498	0.146821	1.983084	2.034492
10	134.111	0.065617	0.883341	0.142161	1.972731	2.299362
12.5	134.111	0.082021	0.882974	0.142896	2.274664	2.291139
15	134.111	0.098425	0.885388	0.138535	1.995939	2.086017
17.5	134.111	0.114829	0.889585	0.128939	2.13536	2.083022
20	134.111	0.131234	0.896189	0.130413	2.353724	2.257985
22.5	134.111	0.147638	0.908269	0.126972	2.58745	2.329922
25	134.111	0.164042	0.917781	0.134035	2.929981	2.420929
27.5	134.111	0.180446	0.932847	0.128004	3.250868	2.486847
30	134.111	0.19685	0.957238	0.126573	3.077691	2.812721
32.5	134.111	0.213255	0.968656	0.140418	4.794605	3.464728
35	134.111	0.229659	0.812302	0.179537	18.0881	6.840618
37.5	134.111	0.246063	0.387421	0.222471	18.76181	16.42505
37.5	134.111	0.246063	0.077288	0.117112	20.14701	19.97381
40	134.111	0.262467	-0.03019	0.013347	12.83388	15.60643
42.5	134.111	0.278871	-0.04694	0.021366	11.51553	14.79738
45	134.111	0.295276	-0.02179	0.033547	12.52125	14.3003
47.5	134.111	0.31168	0.026182	0.069982	17.27535	15.57374
50	134.111	0.328084	0.12987	0.075197	22.8687	15.82149
52.5	134.111	0.344488	0.283865	0.140738	24.27147	15.74352
55	134.111	0.360892	0.407797	0.16033	20.20933	13.45235
57.5	134.111	0.377297	0.476066	0.151003	17.69148	14.44345
60	134.111	0.393701	0.543529	0.163257	17.94157	14.35574
62.5	134.111	0.410105	0.622445	0.195105	18.48655	14.6466
65	134.111	0.426509	0.711488	0.180262	18.48275	13.26777
67.5	134.111	0.442913	0.797121	0.17172	17.32558	11.33636
70	134.111	0.459318	0.877664	0.161324	12.97117	6.443802
72.5	134.111	0.475722	0.920042	0.167783	7.039993	5.683021
75	134.111	0.492126	0.91824	0.166024	5.624034	4.134725
77.5	134.111	0.50853	0.918106	0.156866	4.138796	3.010279
80	134.111	0.524934	0.909924	0.161132	3.384954	2.776882
82.5	134.111	0.541339	0.911405	0.161479	2.833047	2.777117
85	134.111	0.557743	0.900374	0.162886	2.58845	2.346846
87.5	134.111	0.574147	0.89623	0.161268	2.330897	2.150078
90	134.111	0.590551	0.887364	0.165934	2.285335	2.124403
92.5	134.111	0.606955	0.879585	0.172393	2.600266	2.02245
95	134.111	0.62336	0.868582	0.16933	2.569353	2.208045
97.5	134.111	0.639764	0.862216	0.161639	2.749985	2.240892

Station 12 Coarse Grid @ 12" H_2O

U ref = 70.4253

V ref = 71.3758

y (mm)	x (mm)	y/s	U ref	V ref	Tu	Tv
0	134.111	0	0.876485	0.160267	1.731136	2.065604
5	134.111	0.032808	0.884089	0.150246	1.823556	2.060964
10	134.111	0.065617	0.886447	0.130667	2.417527	2.173846
15	134.111	0.098425	0.890206	0.111132	1.853266	2.167045
20	134.111	0.131234	0.898762	0.091409	1.743024	2.192124
25	134.111	0.164042	0.911148	0.067053	1.803272	1.894673
30	134.111	0.19685	0.911306	0.049288	10.5665	1.704241
35	134.111	0.229659	0.788112	0.001008	11.19158	0.054774
40	134.111	0.262467	0.080462	-0.04918	5.031259	4.439055
45	134.111	0.295276	-0.05293	-0.02599	2.231487	5.84764
50	134.111	0.328084	0.031839	0.042796	3.798599	10.97162
55	134.111	0.360892	0.281115	0.144821	64.98814	15.17447
60	134.111	0.393701	0.447512	0.291798	29.29005	9.979572
65	134.111	0.426509	0.553594	0.337939	16.14606	7.662879
70	134.111	0.459318	0.698072	0.316072	27.3746	7.801829
75	134.111	0.492126	0.890231	0.263959	3.725751	7.042986
80	134.111	0.524934	0.90855	0.221603	2.046336	4.071027
85	134.111	0.557743	0.906666	0.210912	1.814582	2.681153
90	134.111	0.590551	0.89967	0.203737	2.063518	2.325394
95	134.111	0.62336	0.886904	0.196764	2.219655	2.73028
100	134.111	0.656168	0.867059	0.187699	2.367635	2.712126
105	134.111	0.688976	0.847873	0.180169	2.338264	2.750729
110	134.111	0.721785	0.837005	0.165528	2.059157	2.031907
115	134.111	0.754593	0.830331	0.160018	2.19219	1.874593
120	134.111	0.787402	0.833771	0.15648	2.138824	1.71651
125	134.111	0.82021	0.8349	0.152564	2.066745	1.694822
130	134.111	0.853018	0.836211	0.147959	2.280589	1.874923
135	134.111	0.885827	0.831428	0.141381	2.107305	1.890013
140	134.111	0.918635	0.826217	0.133362	2.143472	1.856616
145	134.111	0.951444	0.822618	0.125142	1.967381	1.893809
150	134.111	0.984252	0.824401	0.116138	2.04477	1.828711
155	134.111	1.01706	0.83431	0.107327	2.263465	1.921239
160	134.111	1.049869	0.848505	0.094704	1.934031	2.074853
165	134.111	1.082677	0.86668	0.082903	2.154359	2.089123
170	134.111	1.115486	0.887461	0.077663	2.282026	2.561768
175	134.111	1.148294	0.901933	0.064722	2.268578	2.427156
180	134.111	1.181102	0.913426	0.0559	4.218064	6.010677
185	134.111	1.213911	0.905037	0.049191	12.99669	0.840166
190	134.111	1.246719	0.350773	-0.03191	2.105389	2.820415
195	134.111	1.279528	-0.04549	-0.00628	0.24862	0.473523
200	134.111	1.312336	-0.00985	0.038351	0.59197	0.635716
205	134.111	1.345144	0.138182	0.135316	15.55297	2.461672
210	134.111	1.377953	0.401251	0.233254	93.61299	16.12889
215	134.111	1.410761	0.472955	0.319124	35.54295	9.978515
220	134.111	1.44357	0.595694	0.329306	18.46579	8.760371
225	134.111	1.476378	0.801955	0.299838	8.268474	7.742545
230	134.111	1.509186	0.894784	0.255665	5.211166	4.867633
235	134.111	1.541995	0.905205	0.226961	2.148014	3.034669
240	134.111	1.574803	0.903411	0.216533	1.75428	2.167883
245	134.111	1.607612	0.898765	0.209679	1.703681	2.037121

Station 12 Fine Grid @ 12" H$_2$O

U ref = 70.2472

V ref = 70.3211

y (mm)	x (mm)	y/s	U ref	V ref	Tu	Tv
0	134.111	0	0.87837	0.168949	1.647039	1.804851
2.5	134.111	0.016404	0.880599	0.16347	1.424069	1.801327
5	134.111	0.032808	0.880503	0.16097	1.344573	2.020369
7.5	134.111	0.049213	0.882381	0.159589	1.467453	2.088243
10	134.111	0.065617	0.88625	0.151893	1.379404	1.999219
12.5	134.111	0.082021	0.885382	0.144577	1.430361	2.213746
15	134.111	0.098425	0.890985	0.14118	1.426244	2.396114
17.5	134.111	0.114829	0.895956	0.135937	1.474941	2.518812
20	134.111	0.131234	0.900638	0.132666	1.406878	2.381188
22.5	134.111	0.147638	0.906653	0.126372	1.522478	2.540476
25	134.111	0.164042	0.909668	0.117904	1.711494	2.963273
27.5	134.111	0.180446	0.915537	0.12081	1.954232	2.975729
30	134.111	0.19685	0.916103	0.110505	2.030131	3.453846
32.5	134.111	0.213255	0.909067	0.114239	2.422218	4.007908
35	134.111	0.229659	0.737644	0.198517	16.47866	8.964053
37.5	134.111	0.246063	0.417137	0.304817	10.86304	13.7843
37.5	134.111	0.246063	0.099684	0.100965	18.36456	17.8784
40	134.111	0.262467	0.000887	0.020574	12.27074	12.61044
42.5	134.111	0.278871	-0.05678	0.000411	5.115539	9.996287
45	134.111	0.295276	-0.00753	0.023406	11.35233	11.33518
47.5	134.111	0.31168	0.076337	0.053696	17.12145	13.91365
50	134.111	0.328084	0.185754	0.108356	19.96893	16.41755
52.5	134.111	0.344488	0.360682	0.160188	12.48941	16.8622
55	134.111	0.360892	0.402674	0.213825	10.23564	17.07744
57.5	134.111	0.377297	0.462058	0.287993	11.25371	11.83425
60	134.111	0.393701	0.504459	0.326565	14.22336	9.913105
62.5	134.111	0.410105	0.560447	0.336137	14.94873	8.755184
65	134.111	0.426509	0.648819	0.352172	16.91438	8.263215
67.5	134.111	0.442913	0.718497	0.324477	16.11488	10.8939
70	134.111	0.459318	0.843887	0.30015	8.353697	11.3521
72.5	134.111	0.475722	0.890996	0.251809	3.724071	9.582901
75	134.111	0.492126	0.905297	0.207349	2.19588	6.588634
77.5	134.111	0.50853	0.907112	0.190587	1.983746	4.335553
80	134.111	0.524934	0.908381	0.181782	1.590566	3.287252
82.5	134.111	0.541339	0.907272	0.178359	1.683588	2.858649
85	134.111	0.557743	0.904262	0.1762	1.510471	2.535241
87.5	134.111	0.574147	0.89657	0.17616	1.575156	2.390322
90	134.111	0.590551	0.890971	0.174272	1.704578	2.352184
92.5	134.111	0.606955	0.885752	0.171166	1.910204	2.349291
95	134.111	0.62336	0.873381	0.167748	1.929762	2.309483
97.5	134.111	0.639764	0.861697	0.164982	2.038689	2.587013

Station 13 @ 2" H_2O

U ref = 30.6977

V ref = 32.1817

y (mm)	x (mm)	y/s	U ref	V ref	Tu	Tv
0	134.111	0	0.829486	0.132866	1.414464	1.923521
2.5	134.111	0.016404	0.83462	0.127029	1.473404	1.916538
5	134.111	0.032808	0.833945	0.124924	1.444001	1.878646
7.5	134.111	0.049213	0.837643	0.119213	1.477417	2.17946
10	134.111	0.065617	0.837584	0.118208	1.445854	2.072142
12.5	134.111	0.082021	0.840213	0.131793	1.563779	2.422551
15	134.111	0.098425	0.840959	0.131804	1.554243	2.28905
17.5	134.111	0.114829	0.845083	0.130215	1.690647	2.354047
20	134.111	0.131234	0.844907	0.130934	1.939205	2.369914
22.5	134.111	0.147638	0.844154	0.116011	2.118726	2.795628
25	134.111	0.164042	0.840402	0.120139	2.258462	3.210665
27.5	134.111	0.180446	0.846487	0.138236	3.099793	3.555762
30	134.111	0.19685	0.84505	0.134376	4.280281	4.371603
32.5	134.111	0.213255	0.849018	0.171308	6.151263	6.002687
35	134.111	0.229659	0.834919	0.174205	9.701845	7.436459
37.5	134.111	0.246063	0.597706	0.175228	18.67	13.78659
37.5	134.111	0.246063	0.327334	0.206774	14.43117	19.29459
40	134.111	0.262467	0.328363	0.094533	17.83801	16.22937
42.5	134.111	0.278871	0.446053	0.056103	25.56628	11.74977
45	134.111	0.295276	0.582825	0.035155	26.13855	12.56702
47.5	134.111	0.31168	0.775374	0.048695	10.40164	12.28703
50	134.111	0.328084	0.804187	0.038654	7.549887	7.044856
52.5	134.111	0.344488	0.826616	0.033063	4.765638	4.637907
55	134.111	0.360892	0.828645	0.038894	4.856523	3.963018
57.5	134.111	0.377297	0.834111	0.049314	4.44603	4.307999
60	134.111	0.393701	0.841451	0.056852	4.459133	1.764544
62.5	134.111	0.410105	0.840522	0.061939	2.247901	2.191895
65	134.111	0.426509	0.839695	0.070497	1.910558	1.739321
67.5	134.111	0.442913	0.839744	0.076366	2.066231	1.774076
70	134.111	0.459318	0.839968	0.08292	1.906031	1.783014
72.5	134.111	0.475722	0.84018	0.08202	2.051863	1.691019
75	134.111	0.492126	0.837665	0.090083	1.939664	1.609082
77.5	134.111	0.50853	0.835796	0.092721	1.653195	1.584245
80	134.111	0.524934	0.830935	0.104009	1.582416	1.593056
82.5	134.111	0.541339	0.833649	0.105546	1.607033	1.904082
85	134.111	0.557743	0.830952	0.114216	1.643888	1.985288
87.5	134.111	0.574147	0.82817	0.117235	1.585605	1.512718
90	134.111	0.590551	0.826704	0.11432	1.475352	1.600944
92.5	134.111	0.606955	0.825554	0.115304	1.385882	1.49115
95	134.111	0.62336	0.818993	0.118231	1.598732	1.510415
97.5	134.111	0.639764	0.818179	0.117119	1.454337	1.523688

Station 13 @ 8" H_2O

	U ref =	57.5636				
	V ref =	57.6576				
y (mm)	x (mm)	y/s	U ref	V ref	Tu	Tv
0	146.304	0	0.866106	0.170957	1.799864	1.847308
2.5	146.304	0.016404	0.869789	0.169473	1.80249	1.920795
5	146.304	0.032808	0.873715	0.173308	1.879851	2.112611
7.5	146.304	0.049213	0.877327	0.172778	1.81547	2.032598
10	146.304	0.065617	0.877049	0.171943	2.048287	2.306134
12.5	146.304	0.082021	0.876328	0.167917	2.150895	2.16883
15	146.304	0.098425	0.879764	0.170239	2.068651	2.291691
17.5	146.304	0.114829	0.878156	0.169659	2.024184	2.323749
20	146.304	0.131234	0.881222	0.170346	2.237607	2.468788
22.5	146.304	0.147638	0.887601	0.173713	2.602605	2.313064
25	146.304	0.164042	0.88767	0.178391	2.648746	2.975081
27.5	146.304	0.180446	0.888511	0.189907	3.157387	3.236628
30	146.304	0.19685	0.890509	0.196649	4.270418	4.511498
32.5	146.304	0.213255	0.88898	0.227653	5.279289	5.94139
35	146.304	0.229659	0.849547	0.25667	7.968499	7.360127
37.5	146.304	0.246063	0.728605	0.330133	12.87182	11.91072
37.5	146.304	0.246063	0.575501	0.327164	14.08279	16.9205
40	146.304	0.262467	0.445384	0.317667	13.39839	18.07689
42.5	146.304	0.278871	0.339925	0.25764	21.17671	19.1637
45	146.304	0.295276	0.387611	0.200319	27.79456	20.84998
47.5	146.304	0.31168	0.511916	0.166957	26.82033	20.09858
50	146.304	0.328084	0.467523	0.131518	21.52433	21.05479
52.5	146.304	0.344488	0.548553	0.160773	16.93329	19.46562
55	146.304	0.360892	0.58439	0.151075	16.98179	17.95569
57.5	146.304	0.377297	0.617826	0.161812	16.64362	17.97688
60	146.304	0.393701	0.658156	0.172996	15.37576	17.14679
62.5	146.304	0.410105	0.739943	0.144834	13.33393	14.40525
65	146.304	0.426509	0.788069	0.123373	10.76353	12.07888
67.5	146.304	0.442913	0.824233	0.129829	8.983477	11.74877
70	146.304	0.459318	0.864982	0.114766	6.161616	7.86754
72.5	146.304	0.475722	0.866092	0.11984	6.105216	6.394063
75	146.304	0.492126	0.881413	0.124835	4.459341	5.118751
77.5	146.304	0.50853	0.871641	0.131696	3.760408	4.469819
80	146.304	0.524934	0.877146	0.13666	3.355743	4.075583
82.5	146.304	0.541339	0.873017	0.131409	2.973679	2.876658
85	146.304	0.557743	0.869602	0.145026	2.502331	2.879295
87.5	146.304	0.574147	0.869437	0.150141	2.344192	2.573471
90	146.304	0.590551	0.86386	0.146347	2.212139	2.266348
92.5	146.304	0.606955	0.856995	0.154329	2.286299	2.190482
95	146.304	0.62336	0.85728	0.154247	2.082555	2.150617
97.5	146.304	0.639764	0.848524	0.152682	2.412422	2.369879

Station 13 Coarse Grid @ 12" H₂O
  U ref = 70.1014
  V ref = 70.0618

y (mm)	x (mm)	y/s	U ref	V ref	Tu	Tv
0	146.304	0	0.873322	0.169094	2.076681	1.819193
5	146.304	0.032808	0.873793	0.174577	2.313987	1.972357
10	146.304	0.065617	0.878525	0.169058	2.180586	2.106664
15	146.304	0.098425	0.876375	0.17443	2.306627	2.269478
20	146.304	0.131234	0.880373	0.174946	2.554306	2.120602
25	146.304	0.164042	0.88476	0.180182	2.556195	2.945387
30	146.304	0.19685	0.869888	0.194173	4.001026	3.996932
35	146.304	0.229659	0.792432	0.234443	6.846542	7.790917
40	146.304	0.262467	0.622766	0.235125	10.73176	13.0389
45	146.304	0.295276	0.576101	0.157258	15.75239	16.64815
50	146.304	0.328084	0.154488	0.078079	13.5025	15.702
55	146.304	0.360892	0.231753	0.07727	13.1596	13.19541
60	146.304	0.393701	0.322536	0.08793	13.57811	13.46836
65	146.304	0.426509	0.595079	0.119401	11.34555	11.4732
70	146.304	0.459318	0.69026	0.135039	8.887996	10.10395
75	146.304	0.492126	0.750998	0.132696	6.860718	6.650497
80	146.304	0.524934	0.797719	0.128069	6.948689	3.93126
85	146.304	0.557743	0.838488	0.139098	5.623934	2.734203
90	146.304	0.590551	0.868228	0.151884	3.420063	2.279999
95	146.304	0.62336	0.870943	0.152728	2.730693	1.995605
100	146.304	0.656168	0.860579	0.153554	2.689903	1.998603
105	146.304	0.688976	0.85091	0.157921	2.676734	2.151478
110	146.304	0.721785	0.826069	0.146835	2.69771	2.513795
115	146.304	0.754593	0.810348	0.134172	2.420322	2.027126
120	146.304	0.787402	0.804596	0.136915	2.342299	1.94307
125	146.304	0.82021	0.802328	0.130221	2.185469	1.802032
130	146.304	0.853018	0.806356	0.133486	2.126095	1.570828
135	146.304	0.885827	0.814713	0.13496	2.318338	1.678847
140	146.304	0.918635	0.819808	0.13432	2.164843	1.776355
145	146.304	0.951444	0.813667	0.13335	2.163996	1.719961
150	146.304	0.984252	0.806503	0.127372	2.325318	1.835146
155	146.304	1.01706	0.809496	0.126148	2.056816	1.811385
160	146.304	1.049869	0.817915	0.125813	2.130694	1.768129
165	146.304	1.082677	0.822412	0.128355	2.205371	2.004474
170	146.304	1.115486	0.837811	0.135316	2.277203	2.261373
175	146.304	1.148294	0.853357	0.142689	2.446096	2.802504
180	146.304	1.181102	0.873318	0.164181	2.637961	3.739874
185	146.304	1.213911	0.870249	0.205546	3.576029	6.104707
190	146.304	1.246719	0.826139	0.241515	5.838985	11.75443
195	146.304	1.279528	0.665192	0.184143	10.97387	13.44442
200	146.304	1.312336	0.288749	0.111622	14.94541	14.96591
205	146.304	1.345144	0.282552	0.105593	14.7145	10.59705
210	146.304	1.377953	0.693584	0.066848	7.46643	13.42367
215	146.304	1.410761	0.216599	0.101255	13.39126	11.58933
220	146.304	1.44357	0	0.136119	0	12.22267
225	146.304	1.476378	0.56521	0.140631	12.40681	10.14518
230	146.304	1.509186	0.6293	0.139957	11.5109	7.840748
235	146.304	1.541995	0.707746	0.138158	8.98406	4.505826
240	146.304	1.574803	0.768447	0.149302	7.041125	3.535259
245	146.304	1.607612	0.818965	0.149909	6.198124	2.267225

Station 13 Fine Grid @ 12" H$_2$O

U ref = 70.3144

V ref = 70.3803

y (mm)	x (mm)	y/s	U ref	V ref	Tu	Tv
0	146.304	0	0.887372	0.167436	1.242471	1.697165
2.5	146.304	0.016404	0.889577	0.169893	1.242197	1.634663
5	146.304	0.032808	0.887454	0.173341	1.438678	1.937538
7.5	146.304	0.049213	0.893439	0.173358	1.265529	1.906888
10	146.304	0.065617	0.891314	0.168618	1.525154	1.975868
12.5	146.304	0.082021	0.893264	0.167699	1.370168	2.053423
15	146.304	0.098425	0.894074	0.166326	1.375417	2.16201
17.5	146.304	0.114829	0.896304	0.172335	1.4185	2.088909
20	146.304	0.131234	0.897665	0.174829	1.379945	2.349087
22.5	146.304	0.147638	0.899105	0.176302	1.610215	2.410086
25	146.304	0.164042	0.901037	0.184627	1.692545	2.975503
27.5	146.304	0.180446	0.899931	0.189478	1.858924	3.132351
30	146.304	0.19685	0.89448	0.197149	2.168568	4.284716
32.5	146.304	0.213255	0.880997	0.212123	3.173361	5.76428
35	146.304	0.229659	0.833653	0.237799	7.365848	7.619595
37.5	146.304	0.246063	0.64908	0.265132	15.12143	9.596548
37.5	146.304	0.246063	0.475565	0.235378	11.46631	13.42862
40	146.304	0.262467	0.379449	0.205271	10.58472	12.49847
42.5	146.304	0.278871	0.232578	0.18063	19.08739	12.54129
45	146.304	0.295276	0.13819	0.148002	18.37037	12.25559
47.5	146.304	0.31168	0.114653	0.128484	17.93261	11.68315
50	146.304	0.328084	0.171985	0.120825	19.10079	10.81778
52.5	146.304	0.344488	0.300004	0.124704	17.82432	10.61572
55	146.304	0.360892	0.384001	0.134237	11.79559	9.569906
57.5	146.304	0.377297	0.433172	0.143284	11.81116	9.797831
60	146.304	0.393701	0.453072	0.149941	11.81807	9.914061
62.5	146.304	0.410105	0.511569	0.157061	12.64477	11.12862
65	146.304	0.426509	0.577537	0.14796	14.50751	9.295866
67.5	146.304	0.442913	0.669009	0.139572	16.12025	8.749291
70	146.304	0.459318	0.729465	0.127698	15.03056	5.852001
72.5	146.304	0.475722	0.834148	0.123724	8.071706	5.297409
75	146.304	0.492126	0.868521	0.127833	4.261639	4.807017
77.5	146.304	0.50853	0.884203	0.130025	2.652963	3.691362
80	146.304	0.524934	0.887625	0.134662	2.310354	3.021552
82.5	146.304	0.541339	0.886117	0.141916	2.031078	2.745183
85	146.304	0.557743	0.890028	0.142507	1.729957	2.292627
87.5	146.304	0.574147	0.886486	0.149663	1.878117	2.371793
90	146.304	0.590551	0.880926	0.149724	1.875307	2.033308
92.5	146.304	0.606955	0.878848	0.149719	1.785838	2.143264
95	146.304	0.62336	0.871183	0.151734	1.902393	2.107907
97.5	146.304	0.639764	0.860545	0.153728	2.238802	2.096661

THIS PAGE INTENTIONALLY LEFT BLANK

LIST OF REFERENCES

1. Hansen, D.J., "Investigation of Second Generation Controlled-Diffusion Compressor Blades in Cascade", Master's Thesis, Naval Postgraduate School, Monterey, California, September 1995.

2. Schnorenberg, D.G., "Investigation of Second Generation Controlled-Diffusion Compressor Blades In Cascade", Master's Thesis, Naval Postgraduate School, Monterey, California, June 1996.

3. Grove, D.V., "Experimental and Numerical Investigation of Second-Generation, Controlled-Diffusion Compressor Blades in Cascade", Master's Thesis, Naval Postgraduate School, Monterey, California, June, 1997.

4. Nicholls, J.L., "Investigation of Flow Over Second-Generation Controlled-Diffusion Blades in a Linear Cascade", Master's Thesis, Naval Postgraduate School, Monterey, California, September 1999.

5. Carlson, J.R., "Experimental and Computational Investigation of the End Wall Flow in a Cascade of Compressor Blades", Master's Thesis, Naval Postgraduate School, Monterey, California, September 2000.

6. Caruso, T.M., "Three-Component LDV Measurements of Corner Vertices Over Second Generation Controlled-Diffusion, Compressor Blades in Cascade", Master's Thesis, Naval Postgraduate School, Monterey, California, September 2001.

7. Fitzgerald, K.D., "Examination of Flow Around Second-Generation Controlled-Diffusion Compressor Blades in Cascade at Stall", Master's Thesis, Naval Postgraduate School, Monterey, California, June 2004.

8.   Lim, C.P., "Experimental Investigation of Vortex Shedding in High Reynolds Number Flow Over Compressor Blades in Cascade", Master's Thesis, Naval Postgraduate School, Monterey, California, March 2003.

INITIAL DISTRIBUTION LIST

1. Defense Technical Information Center
    Ft. Belvoir, VA

2. Dudley Knox Library
    Naval Postgraduate School
    Monterey, CA

3. Professor Garth V. Hobson
    Department of Mechanical and Astronautical Engineering
    Code ME/Hg
    Naval Postgraduate School
    Monterey, CA,

4. Professor Knox T. Millsaps
    Department of Mechanical and Astronautical Engineering
    Code ME/Mi
    Naval Postgraduate School
    Monterey, CA,

5. Michael Glova
    Monterey, CA